PHILOSOPHICAL TRANSACTIONS OF THE ROYAL SOCIETY A MATHEMATICAL, PHYSICAL & ENGINEERING SCIENCES

On the Noise Generated by an Imperfectly Expanded Supersonic Jet

M. S. Howe and J. E. Ffowcs Williams

Phil. Trans. R. Soc. Lond. A 1978 **289**, 271-314
doi: 10.1098/rsta.1978.0061

ON THE NOISE GENERATED BY AN IMPERFECTLY EXPANDED SUPERSONIC JET

By M. S. HOWE† and J. E. FFOWCS WILLIAMS
University Engineering Department, Trumpington Street, Cambridge, CB2, 1PZ, U.K.

(*Communicated by Sir Stanley Hooker, F.R.S. – Received 26 May 1977*)

CONTENTS

† Present address: Bolt Beranek and Newman Inc., 50 Moulton Street, Cambridge, Massachusetts 02138, U.S.A.

Vol. 289. A 1358. 20 [Published 2 May 1978

This paper examines in detail a theoretical model describing the generation of sound by an imperfectly expanded supersonic jet. Such a jet consists of a steady system of 'shock cells', and sound is produced by their interaction with turbulence convected in the mixing region of the jet. The dominant convection velocity of the large-scale eddies is shown to be a principal factor determining the total radiated sound power, essentially independently of the details of the interaction mechanism. The ideal laminar jet constitutes a wave guide in which are trapped the steady waves of a super-critical flow. Imperfections of the wave guide cause it to leak. Turbulence provides those imperfections and thus acts as a catalyst enabling the energy of the nominally steady wave system to leak out as sound. When appropriately viewed, the sound power is equal to the power of the wave system in the steady jet. The computation of that power is consequently insensitive to details of the jet turbulence. The spectrum of the sound is characterized by a sequence of peaks produced by coherent scattering from the ends of successive cells. In addition, the theory reveals the existence of a more broadband component which is related to the effects of multiple scattering. The directivity of the radiated sound predicted from the model exhibits encouraging agreement with experiment. The total sound power associated with the presence of the system of shock cells is estimated and shown to be between 0.2 and 1.2 % of the jet exhaust power for a jet operating under conditions appropriate to those of a supersonic transport at take-off. This is entirely consistent with available experimental evidence.

1. Introduction

The mechanism of sound generation by a supersonic air jet differs considerably from the quadrupole sources of the classical theory of aerodynamic noise (Lighthill 1952) in which the turbulent eddies are small on a wavelength scale. A principal component of the jet noise of a supersonic transport such as *Concorde* is produced by the convection at supersonic velocities of large scale turbulent eddies (Bishop, Ffowcs Williams & Smith 1971). These eddies arise from the instability of the primary flow, and the sound they generate is in the form of ballistic shock waves which dominates the field radiated at about 50° to the jet axis.

In practice the supersonic jet is distinguished from the subsonic in that there is usually a difference between the static pressure within the jet and that in the ambient atmosphere. The jet is then said to be imperfectly expanded. The rapid variation in the pressure across the nozzle is accomplished by means of steady compression or expansion waves that trail downstream of the nozzle lip; subsequent multiple internal reflections at the boundary of the jet produce a characteristic system of 'shock-cells'. The structure of these cells was first investigated by Emden (1899), Prandtl (1904) and Rayleigh (1916), and more recently by Pack (1950) and Grabitz (1975). Powell (1953) demonstrated that their presence is responsible for a source of noise usually termed 'screech'. This consists of a discrete spectrum of harmonically related tones, and is generated by an acoustic feedback in which sound which is emitted from the ends of shock cells through an interaction with a turbulent eddy propagates upstream in the ambient medium and releases a new eddy at the nozzle exit. The feedback loop is easily broken, however, and, especially in hot jets, screech is not usually significant.

When the system of shock cells is sufficiently extensive, the interaction of turbulence with the accompanying periodic variations in the flow properties of the jet produces an additional broadband but strongly peaked spectral distribution of sound. This is known as 'shock associated noise'. It has been examined experimentally by Harper Bourne & Fisher (1973); they have also posed an effective empirical modelling of the phenomenon. They show that over a wide range of conditions the intensity of the radiation is a function of the pressure ratio of the jet alone, and in particular does not appear to depend on the stagnation temperature or the jet efflux velocity.

PHILOSOPHICAL TRANSACTIONS OF THE ROYAL SOCIETY A MATHEMATICAL, PHYSICAL & ENGINEERING SCIENCES

Harper Bourne & Fisher considered a large number of experimental configurations and developed a general noise prediction scheme by extending a model originally proposed by Powell (1953) for the treatment of screech. The end of each shock cell was taken to be an omni-directional source of acoustic waves triggered by the passage of a turbulent eddy, the relative phasing of the sources being determined by the average convection velocity of the turbulence. The characteristic peaks of the noise spectrum indicate that acoustic sources at successive shock cells are strongly correlated and therefore that the lifetime of a typical eddy is sufficiently long for it to interact with a substantial number of shock cells.

In this paper an analytical theory of shock associated noise is described in terms of an idealized modelling of a turbulent, imperfectly expanded supersonic jet. The dominant turbulent inhomogeneities are modelled by a continuum of axisymmetric vortex rings of randomly variable strength whose cores are located within a thin mixing layer. The lifetime of an eddy is taken to be great enough that the eddy may be assumed to be 'frozen' as it convects along the jet, and the equations of aerodynamic sound are used to analyse the interactions of the vortex rings with the steady wave system of the coherent cell structure. The procedure constitutes a generalization of Lighthill's (1953) application of his acoustic analogy theory of aerodynamic sound to the scattering of a sound wave by turbulence.

Thus, since the turbulence is frozen, the model describes a situation in which energy is extracted from the ordered non-uniform mean flow of the jet and reappears in the form of random, scattered disturbances. The scattered field comprises two essentially distinct components. The first consists of sound waves which escape directly into free space and give rise to the spectral peaks of the shock associated noise observed by Harper Bourne & Fisher (1973). In addition, however, a random distribution of eigenmodes of the jet is generated which propagate along the jet and whose amplitudes decay exponentially with radial distance from the jet axis. These internally scattered disturbances are distributed over a wide range of frequencies and, because they are confined to the jet, necessarily experience incoherent multiple interactions with the turbulent field. The additional sound waves produced through multiple scattering form a rather broadband component of the free space radiation, a feature of shock associated noise which does not appear to have been appreciated hitherto. This is apparently related to the so-called 'parametric amplification' of jet noise observed in other contexts (Moore 1977).

The loss of energy from the mean flow through these interactions with the turbulent field results in a gradual decay of the coherent shock cell structure with distance downstream of the nozzle. A difficulty arises in attempting to describe this in terms of a transfer of energy from the coherent waves to the random field, essentially because the steady system of shock and expansion waves within the jet constitutes an integral part of the supersonic flow and is not therefore associated with a flux of energy other than that of the total flow. For the same reason, the energy flux cannot be predicted by taking the difference between the mean fluxes along the jet at the nozzle and far downstream where the shocks may be assumed to have disappeared, since these will be identical unless specific account is taken of the manner in which energy is lost during interactions with the turbulence.

Nevertheless, it is convenient to be able to assign a definite value to the energy flux into the coherent wave system at the nozzle exit. This can be done by choosing a reference frame which is in uniform motion parallel to the nozzle. If, further, the velocity of translation of the reference frame is equal to that at which the dominant turbulent eddies are convected along the jet, it also follows that the frozen turbulence becomes independent of the time. This in turn implies that,

with respect to this moving frame of reference, all of the energy which enters the coherent structure at the nozzle is converted into sound and trapped internal waves.

The physical situation in a real jet is different, of course. We have taken no account in the above discussion of the gradual entrainment of ambient fluid by the jet. This causes a progressive reduction in the centre-line jet velocity, which must ultimately become subsonic. When this occurs the jet can no longer support stationary waves and the shock cells must have disappeared. Detailed observations, however (see, for example, Trevett 1968), indicate that the fluctuations in pressure and velocity associated with the cell structure are damped out by the diffusion across the jet of the turbulent mixing region, i.e. through the interaction of the coherent wave system with turbulent inhomogeneities, and that this occurs before the centre-line velocity has become subsonic. Hence we shall assume in our modelling of the problem that the decay of the coherent structure is due entirely to interactions with the turbulent field, the decay being the result of an effective turbulent viscosity.

A purely analytical treatment of this physical problem is tractable only when certain simplifications are introduced into the equations of motion. Pack (1950) has compared experimental data of *underexpanded* jets with predictions of the coherent jet structure based on a linearization of the equations with respect to the degree of non-uniformity in the imperfectly expanded flow. He concludes that in the vicinity of the jet boundary, linear theory provides an accurate description of the flow even for moderate values of the ratio of the excess pressure of the jet at the nozzle exit to the pressure in the ambient atmosphere. Since the interaction between the shock cells and the turbulence occurs mainly in the mixing region of the jet, it may therefore be argued that a linear-theory description of the structure of the shock cells would be expected to yield a valuable first approximation to the scattering problem. (The excess pressure ratio occurring, for example, in the *Concorde* supersonic transport is typically in the range 0.3–0.6.) In fact, we shall neglect all terms which are nonlinear in the irregularities of the flow produced by imperfect expansion, but retain the principal nonlinear components of the equations which account for the interaction between the coherent wave system and the turbulence.

In doing this, a philosophical difficulty is encountered which is currently a subject of debate in the literature. This concerns the basic instability of the jet, and in particular the rôle played by those instabilities which arise in an analysis based on a linearization of the wave propagation operators. In a forthcoming paper, Dowling, Ffowcs Williams & Goldstein (1978) advance convincing theoretical arguments to the effect that these instabilities must be explicitly suppressed when Lighthill's acoustic analogy theory is used to investigate the sound generated by the jet. Analytically this leads to a representation of the acoustic field which satisfies the Sommerfeld radiation condition of outgoing waves at infinity, but not necessarily the causality condition, so that an acoustic disturbance may anticipate the turbulent sources. This is because an aerodynamic source can also initiate the development of new turbulent eddies, and the theory must allow for the prior existence of sound waves associated with the growth of these eddies.

We shall apply this form of reasoning in the present discussion, and ignore possible contributions of unstable solutions to the acoustic analogy equations. Real instabilities are responsible for the growth of the turbulent shear layer. Having recognized that this occurs in the real jet, however, the experimental observation (Harper Bourne & Fisher 1973) that a typical eddy interacts coherently with several shock cells suggests that the essential dynamics of the scattering problem are none the less contained within our model in which the dominant turbulent eddies are assumed to be 'frozen'.

In § 2 of this paper the model problem is defined and those results are obtained from the classical theory of imperfectly expanded supersonic jet flow which will be required in subsequent sections of the paper. The acoustic analogy equations describing the interaction between the turbulence and the shock-cells are formulated in § 3. Their analysis in §§ 4, 5 leads to a description (§ 6) of the coherent cell structure in the presence of the turbulent shear layer. The geometry of the model jet complicates the details of the analysis and for this reason it is initially convenient to confine attention to the idealized situation in which the shear layer is assumed to be infinitely thin. In § 7 the analytical results for this case are interpreted, particular attention being given to the energy balance between the coherent wave system and the randomly scattered disturbances. The spectral properties of the shock-associated noise are deduced in § 8. In § 9 the theory is extended to deal with the case of small but finite shear layer width.

The paper concludes (§ 10) with a numerical application of the theory to the shock associated noise generated by the Rolls Royce–SNECMA *Olympus* 593 engine which powers the *Concorde* supersonic transport. Predicted spectra and directivity of the radiated sound are compared with available experimental data, and the modifications expected from subsonic forward flight of the aircraft are described. Finally an estimate is made of the total radiated sound power arising from the presence of shock cells in the jet.

The principal implications of the present theory are summarized in § 11.

2. Survey of the classical theory of an imperfectly expanded supersonic jet: definition of the model problem

(*a*) *Linear theory of the shock cell structure*

A circular cylindrical jet of density ρ_1 and sound speed c_1 exhausts at velocity U from a semi-infinite cylindrical nozzle of radius a. The motion is axi-symmetric and is referred to a system of cylindrical polar coordinates (x_1, r, φ) the x_1 -axis lying along the centre-line of the jet with U in the positive x_1 direction. The nozzle extends between $x_1 = -\infty$ and the origin (see figure 1*a*). The fluid in free space is at rest relative to the nozzle, with density and sound speed respectively equal to ρ_0, c_0.

The jet velocity U is supersonic, i.e.

$$M_J \equiv U/c_1 > 1.$$

Let there be an excess pressure P (positive or negative) in the jet at the nozzle exit with respect to the pressure in the ambient atmosphere. This situation is characteristic of an imperfectly expanded nozzle flow (see, for example, Liepmann & Roshko 1957, p. 127), and the rapid variation in the mean pressure which must occur at the nozzle exit is accommodated by a system of steady waves emanating from the nozzle lip. The cell-like structure of the jet arises from the subsequent multiple internal reflections of this system at the boundaries of the jet.

In the classical theory (see Pack 1950) it is assumed that P is sufficiently small for the jet flow to be described by the linearized equations of motion. For an ideal fluid, axisymmetric perturbations in the pressure p within the jet satisfy the convected wave equation

$$\frac{1}{c_1^2}\left(\frac{\partial}{\partial t}+U\frac{\partial}{\partial x_1}\right)^2 p-\frac{\partial^2 p}{\partial x_1^2}-\frac{1}{r}\frac{\partial}{\partial r}\left(r\frac{\partial p}{\partial r}\right)=0. \tag{2.1}$$

Let $\bar{p}$ denote the steady distribution of pressure within the flow. If pressure is reckoned relative to that of the jet upstream of the nozzle, the steady-state solution of (2.1) must satisfy

$$\left.\begin{aligned} \bar{p} &= 0 \quad (x_1 < 0, 0 \leqslant r < a), \\ \bar{p} &= -P \quad (x_1 > 0, r = a). \end{aligned}\right\} \tag{2.2}$$

To solve (2.1) introduce the Fourier x_1-transform $\hat{p}$ of the pressure by means of the definition:

$$\left.\begin{aligned} \hat{p} \equiv \hat{p}(r,k) &= (1/2\pi)\int_{-\infty}^{\infty} p(r,x_1)\,\mathrm{e}^{-\mathrm{i}kx_1}\,\mathrm{d}x_1, \\ p(r,x_1) &= \int_{-\infty}^{\infty} \hat{p}(r,k)\,\mathrm{e}^{\mathrm{i}kx_1}\,\mathrm{d}k. \end{aligned}\right\} \tag{2.3}$$

Then in the case of time-independent flow, the transform of (2.1) becomes

$$\frac{1}{r}\frac{\partial}{\partial r}\left(r\frac{\partial \hat{p}}{\partial r}\right) + \beta_1^2 k^2 \hat{p} = 0, \tag{2.4}$$

where

$$\beta_1 = \sqrt{(M_J^2 - 1)} > 0. \tag{2.5}$$

The solution of (2.4) which remains bounded at $r = 0$ has the form $\hat{p} = A(k)\,J_0(\beta_1 kr)$. Noting that the Fourier transform of the boundary value (2.2) of the pressure is

$$\hat{p} = -P/2\pi\mathrm{i}k, \tag{2.6}$$

it follows that

$$A(k) = \frac{-P}{2\pi\mathrm{i}kJ_0(\beta_1 ka)} \tag{2.7}$$

and hence that the pressure distribution within the jet is given by

$$\bar{p} = \frac{-P}{2\pi\mathrm{i}}\int_{-\infty}^{\infty} \frac{J_0(\beta_1 kr)\,\mathrm{e}^{\mathrm{i}kx_1}\,\mathrm{d}k}{(k - \mathrm{i}\sigma)\,J_0(\beta_1 ka - \mathrm{i}\sigma)}. \tag{2.8}$$

In this formula σ is a small positive quantity which is introduced to make the path of integration pass below all of the singularities of the integrand which would otherwise lie on the real axis. Since $J_0(z)$ is an entire function, this choice of the integration contour ensures that $\bar{p}$ vanishes at all points of the flow upstream of the characteristic surface, $\beta_1(r-a) + x_1 = 0$, which springs from the lip of the nozzle. Downstream the pressure variations within the jet are determined by the poles of the integrand. They give rise to a flow which varies quasi-periodically with distance x_1 and characterize the shock-cells of an imperfectly expanded jet, though of course in this linear theory model there are no real shocks. The form of these cells may be determined from the radial component of the momentum equation. At $r = a$ this becomes

$$\left(\frac{\partial}{\partial t} + U\frac{\partial}{\partial x_1}\right)^2 \eta = -\frac{1}{\rho_1}\frac{\partial p}{\partial r}, \tag{2.9}$$

where η is the radial displacement of the jet boundary from $r = a$, that of an ideally expanded flow. In the present case (2.8), (2.9) imply that

$$\eta \equiv \bar{\eta} = \frac{\beta_1 P}{2\pi\mathrm{i}\rho_1 U^2}\int_{-\infty}^{\infty} \frac{J_1(\beta_1 ka)\,\mathrm{e}^{\mathrm{i}kx_1}\,\mathrm{d}k}{(k - \mathrm{i}\sigma)^2\,J_0(\beta_1 ka - \mathrm{i}\sigma)}. \tag{2.10}$$

The displacement $\bar{\eta}$ vanishes identically upstream of the nozzle ($x_1 < 0$) in accordance with the condition of vanishing normal velocity on the nozzle. For $x_1 > 0$ the shape of the jet is determined

by the poles of the integrand in (2.10). These are located at $k = 0$, and at $\beta_1 ka = \pm \lambda_n$ $(1 < n < \infty)$, where λ_n is the nth positive zero of $J_0(z)$. Evaluating (2.10) by residues, we find that for $x_1 > 0$,

$$\bar{\eta} = \frac{a\beta_1^2 P}{\rho_1 U^2}\left[\tfrac{1}{2} - 2\sum_{n=1}^{\infty}\frac{1}{\lambda_n^2}\cos\left(\frac{\lambda_n x_1}{\beta_1 a}\right)\right]. \tag{2.11}$$

The zeros λ_n of $J_0(z)$ are approximately equally spaced along the positive real axis only for n greater than about 2, and this results in the quasi-periodic cell structure illustrated in figure 1*b* for $\beta_1 = 1$, $P > 0$, (cf. Howarth 1953, p. 319). Also shown are the multiply reflected leading characteristics from the nozzle lip.

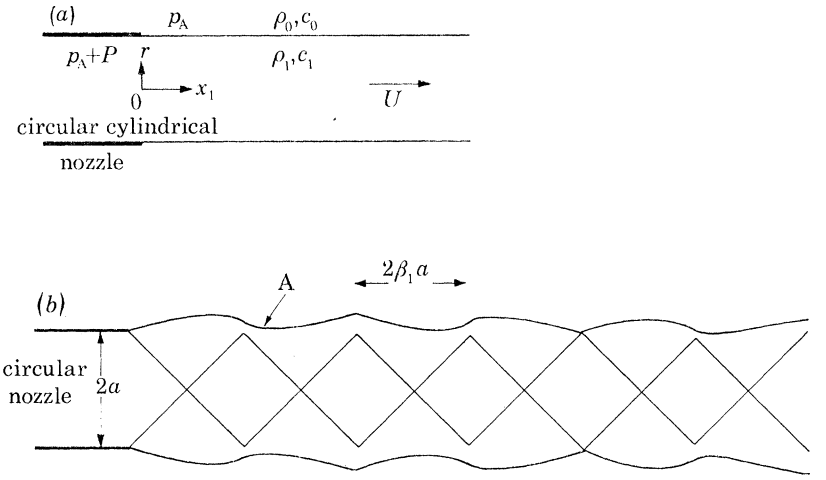

FIGURE 1. (*a*) An idealized circular cylindrical jet of density ρ_1 and sound speed c_1 exhausts at a supersonic velocity U into an ambient medium of density ρ_0 and sound speed c_0. The ambient atmospheric pressure is equal to p_A, and P is the excess pressure in the jet at the nozzle exit plane. (*b*) Illustrating the boundary displacement of the idealized jet for the case in which $\beta_1 \equiv \sqrt{(M_j^2 - 1)} = 1$ $(M_j = U/c_1)$. The point A is the first minimum in the displacement (see §10).

In the above discussion no account has been taken of real fluid properties such as heat conduction and viscosity. Nor have we considered the effect of the turbulent mixing layer which ultimately transforms the simple, laminar regime described above into a fully developed turbulent flow within about ten jet diameters downstream of the nozzle, at which stage the cell structure has effectively disappeared. At the relatively high Reynolds numbers encountered in aeronautical applications, turbulent diffusion is probably the dominant mechanism responsible for the degradation of the cell structure. We have argued in the introduction that this is likely to occur before the centre-line jet velocity has become subsonic, and therefore that the decay is primarily caused by an interaction with the turbulent fluctuations. In this paper we shall confine attention to situations in which other irreversible phenomena may be ignored, at least in as much as their effect on the regular structure of the jet is concerned.

If, further, it is permissible to continue with the linearized approximation, turbulent diffusion will produce a decay in the amplitudes of the harmonic components in (2.11) of the regular or coherent cell structure. The contribution from the summation in (2.11) would then tend to zero as $x_1 \to \infty$, and the asymptotic, fully expanded mean jet radius would be

$$a_\infty = a\left(1 + \frac{\beta_1^2 P}{2\rho_1 U^2}\right). \tag{2.12}$$

The rate at which energy is extracted from each harmonic component through interactions with the turbulence is proportional to the amplitude of that component. This implies an exponential decay with increasing x_1 and if the rate of decay is sufficiently small the effect of turbulent diffusion may be incorporated into the integral representation (2.8), say, of the pressure distribution by writing

$$\bar{p} = \frac{-P}{2\pi \mathrm{i}} \int_{-\infty}^{\infty} \frac{J_0(\beta_1 kr)\, \mathrm{e}^{\mathrm{i}kx_1}\, \mathrm{d}k}{(k - \mathrm{i}\sigma)\, J_0(\beta_1 ka - \mathrm{i}\Delta(k))}, \tag{2.13}$$

where $\Delta(k) > 0$ and $\Delta(k) \ll \beta_1 ka$. Thus the poles of the integrand are displaced into the upper half of the k-plane leading to an exponential decay of the quasi-periodic structure downstream of the nozzle. The *dissipation function* $\Delta(k)$ is a function of the wavenumber k, and is determined by the details of the turbulent fluctuations in the jet. It describes the effect of the continuous transfer of energy from the coherent jet structure, in which waves propagating against the stream are unable to move because of the exactly balancing headwind, into random disturbances which do move, either as trapped waves within the jet or as sound waves which radiate to infinity in the ambient medium. The coherent jet profile (2.11) now becomes

$$\bar{\eta} = \frac{a\beta_1^2 P}{\rho_1 U^2}\left[\tfrac{1}{2} - 2\sum_{n=1}^{\infty} \frac{\mathrm{e}^{-(d_n x_1/\beta_1 a)}}{\lambda_n^2} \cos\left(\frac{\lambda_n x_1}{\beta_1 a}\right)\right], \tag{2.14}$$

where $d_n = \Delta(\lambda_n/\beta_1 a)$.

The internally scattered disturbances will also decay as a result of irreversible processes. If it is still permissible to ignore thermodynamic dissipation, the effect of multiple interactions with the turbulent flow leads ultimately to the conversion of their energy into sound waves in free space. In this limiting case, therefore, all of the perturbation energy associated with the coherent jet structure (see below) eventually radiates away from the jet as sound.

(*b*) *Theoretical modelling of a turbulent jet*

In the subsequent sections of this paper we shall investigate the effect of turbulent diffusion on the decay of the coherent structure in terms of an idealized model problem illustrated in figure 2. In order to make the analysis tractable yet still retain the essential properties of a real jet, it will be assumed that the dominant turbulent fluctuations are confined within a thin shear layer of width δ between the jet flow and the ambient medium. The experimental observations of Davies, Fisher & Barratt (1963) and others indicate that large-scale vortical disturbances within the shear layer convect at a velocity $V \approx 0.6U$. Accordingly our model consists of an inner cylindrical uniform core flow of velocity U and radius a, surrounded by a coannular flow of velocity V and width δ, the interface with the ambient medium being at $r = b \equiv a + \delta$. The mean density and sound speed will be assumed to be constant throughout the jet and shear layer and equal respectively to ρ_1, c_1.

The turbulent fluctuations within the shear layer are modelled by an infinitely thin, axisymmetric distribution of vorticity $\boldsymbol{\omega}(r, x_1, t)$ confined to the surface $r = h$ $(a < h < b)$. The vorticity is assumed to be frozen and to convect at the shear flow velocity V, and is given by

$$\boldsymbol{\omega} = \xi(x_1 - Vt)\, \delta(r - h)\, \boldsymbol{l}, \tag{2.15}$$

where $\boldsymbol{l}$ is a unit vector in the azimuthal direction and $\delta(x)$ is the Dirac delta-function. The vortex lines are thus circles perpendicular to the jet axis, and we shall suppose that the circulation density ξ is a stationary random function of its argument with zero mean.

It will be convenient to conduct the analysis in a reference frame in which the shear layer and the vorticity distribution are at rest. Set

$$x = x_1 - Vt \tag{2.16}$$

then (2.15) becomes

$$\boldsymbol{\omega} = \xi(x)\,\delta(r-h)\,\boldsymbol{l} \tag{2.17}$$

and in figure 2 the velocity of the inner jet is $U-V$, and the ambient flow is at velocity V in the negative x direction.

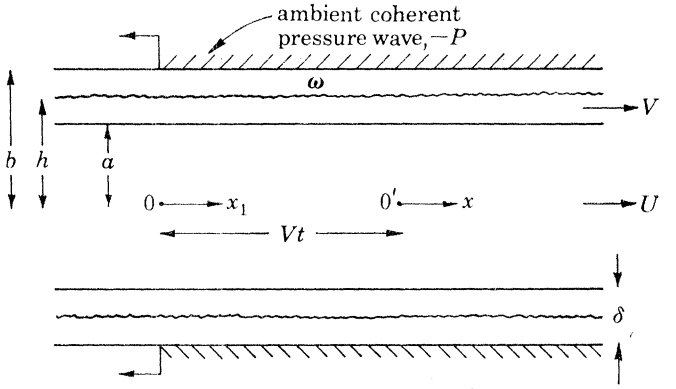

FIGURE 2. Model of a supersonic turbulent jet. The flow in $r < a$ is at a uniform supersonic velocity U. The turbulent fluctuations are condensed into a continuum of idealized vortex rings of radius h, given by (2.15) convected at velocity V in a shear layer of width $\delta = b-a$. The density and sound speed are assumed to be uniform throughout the jet and shear layer, and the nozzle exit is simulated by means of a uniform ambient pressure distribution $-P$ applied at the surface of the jet for $x_1 > 0$.

The circulation density $\xi(x)$ has the dimension of velocity, and we shall assume that the turbulence Mach number,

$$\epsilon = \sqrt{\langle \xi^2 \rangle}/c_1 \ll 1, \tag{2.18}$$

where angle brackets denote an average over an ensemble of realizations of the turbulent fluctuations. The autocorrelation function, $R(x)$, is defined by

$$R(x) = \langle \xi(z)\,\xi(z+x) \rangle \tag{2.19}$$

and its Fourier transform

$$\Phi(k) = (1/2\pi)\int_{-\infty}^{\infty} R(x)\,\mathrm{e}^{-\mathrm{i}kx}\,\mathrm{d}x \tag{2.20}$$

defines the spectrum $\Phi(k)$ of the random function ξ. This is an even, non-negative function of the wavenumber k (see, for example, Stratonovich 1963, p. 27).

The linearized problem of the ideal imperfectly expanded jet of figure 1 was solved by specifying the steady pressure distribution on the jet boundary, the condition of vanishing normal velocity on the nozzle being satisfied identically. We shall adopt the same procedure in the present case, and assume that, in the reference frame which is at rest relative to the shear flow, the coherent pressure distribution on the outer boundary ($r = b$) of the jet is given by

$$\bar{p} = -PH(x+Vt). \tag{2.21}$$

If the shear layer velocity V is supersonic ($V > c_1$) the normal velocity condition at the nozzle will again be satisfied automatically.

(c) *The coherent field power*

In the limit as the shear layer width $\delta = b - a \to 0$ and when turbulent diffusion is neglected, we have seen that the coherent field pressure variations within the jet are given by equation (2.8). In the x-reference frame in which the shear layer is at rest, the ambient pressure perturbation (2.21) propagates to the left in figure 2 and continuously extends the region of the jet flow which is occupied by the coherent wave system. It may therefore be regarded as a source of internal wave energy, the significance of which will emerge below (§7). Let $\mathscr{P}$ denote the corresponding energy flux into the jet.

Now the flux of energy per unit area in the direction of the unit vector $\boldsymbol{n}$ is equal to the mean value of $\rho B\boldsymbol{v}\cdot\boldsymbol{n}$ (Landau & Lifshitz 1959, §6), where $\boldsymbol{v}$ is the fluid velocity and B is the stagnation enthalpy defined by

$$B = w + \tfrac{1}{2}\boldsymbol{v}^2, \tag{2.22}$$

w being the specific enthalpy of the fluid. Hence if $\bar{v}$ denotes the radial component of the coherent field velocity perturbation, and $\bar{B}$ is the corresponding perturbation in the stagnation enthalpy, it follows that, since the mean value of $\rho\bar{v}$ must vanish identically

$$\mathscr{P} = -2\pi a\rho_1 \int_{-\infty}^{\infty} (\bar{v}\bar{B})_{r=a}\,\mathrm{d}x. \tag{2.23}$$

To evaluate this integral note that the flow within the jet is irrotational and isentropic in the absence of dissipative processes, and may therefore be expressed in terms of a potential function $\bar{\phi}$ such that the coherent field velocity $\bar{\boldsymbol{v}} = (\bar{u}, \bar{v}) = (\partial\bar{\phi}/\partial x, \partial\bar{\phi}/\partial r)$. Variations in the fluid density and pressure are related by the 'adiabatic' gas law and we may write

$$w = \int \mathrm{d}p/\rho \approx w_1 + \bar{p}/\rho_1, \tag{2.24}$$

where w_1 is the uniform specific enthalpy of the flow upstream of the nozzle exit. Using this together with Bernoulli's equation (Landau & Lifshitz 1959, §9)

$$\partial\bar{\phi}/\partial t + w + \tfrac{1}{2}[(U - V + \bar{u})^2 + \bar{v}^2] \equiv \partial\bar{\phi}/\partial t + B = \text{const} \tag{2.25}$$

and also the integral representation (2.8), we deduce that in the linearized approximation

$$\left.\begin{aligned} \bar{B} &= \frac{-PV}{2\pi\mathrm{i}\rho_1 U}\int_{-\infty}^{\infty} \frac{\mathrm{e}^{\mathrm{i}k(x+Vt)}}{k - \mathrm{i}\sigma}\,\mathrm{d}k, \\ \bar{v} &= \frac{\beta_1 P}{2\pi\rho_1 U}\int_{-\infty}^{\infty} \frac{J_1(\beta_1 ka)\,\mathrm{e}^{\mathrm{i}k(x+Vt)}}{(k-\mathrm{i}\sigma)\,J_0(\beta_1 ka - \mathrm{i}\sigma)}\,\mathrm{d}k. \end{aligned}\right\} \tag{2.26}$$

These expressions define real functions of $x + Vt$ so that on substitution into (2.23) we have

$$\mathscr{P} = \frac{a\beta_1 P^2 V}{4\pi\rho_1 U^2}\left\{\iiint_{-\infty}^{\infty} \frac{-\mathrm{i}J_1(\beta_1 ka)\,\mathrm{e}^{\mathrm{i}(K-k)(x+Vt)}\,\mathrm{d}K\,\mathrm{d}k\,\mathrm{d}x}{(K-\mathrm{i}\sigma)\,(k+\mathrm{i}\sigma)\,J_0(\beta_1 ka + \mathrm{i}\sigma)} + \text{c.c.}\right\}, \tag{2.27}$$

where 'c.c.' denotes the complex conjugate of the preceding quantity. The integration with respect to x yields $2\pi\delta(K-k)$, after which (2.27) reduces to

$$\mathscr{P} = -\frac{\mathrm{i}a\beta_1 P^2 V}{2\rho_1 U^2}\int_{-\infty}^{\infty}\left[\frac{J_1(\beta_1 ka)}{(k^2+\sigma^2)\,J_0(\beta_1 ka + \mathrm{i}\sigma)} - \text{c.c.}\right]\mathrm{d}k \tag{2.28}$$

As $\sigma \to 0$ the term in square brackets tends to zero unless $\beta_1 ka$ coincides with a zero of $J_0(z)$. To take account of this case we note that for small σ

$$\frac{J_1(\beta_1 ka)}{J_0(\beta_1 ka + i\sigma)} - \text{c.c.} = \frac{J_1(\beta_1 ka)}{|J_0(\beta_1 ka + i\sigma)|^2}\{J_0(\beta_1 ka - i\sigma) - J_0(\beta_1 ka + i\sigma)\}$$
$$\approx \frac{2i\sigma J_1(\beta_1 ka)^2}{|J_0(\beta_1 ka + i\sigma)|^2} \to \sum_{n=-\infty}^{\infty} 2\pi i\, \delta(\beta_1 ka - \lambda_n) \tag{2.29}$$

as $\sigma \to +0$, where for $n > 0$, λ_n is the nth positive zero of $J_0(z)$ introduced above, and for $n < 0$, $\lambda_n \equiv -\lambda_{-n}$. Using (2.29) in (2.28) we finally obtain

$$\mathscr{P} = \frac{2\pi a^2 \beta_1^2 P^2 V}{\rho_1 U^2} \sum_{n=1}^{\infty} \frac{1}{\lambda_n^2}. \tag{2.30}$$

This infinite series representation of the energy flux into the jet determines the distribution of energy amongst the harmonic components which comprise the coherent wave structure of equation (2.11). The infinite series in (2.30) can be evaluated exactly (see Pack 1950), and the sum is equal to $\frac{1}{4}$, so that finally

$$\mathscr{P} = \pi a^2 \beta_1^2 P^2 V / 2\rho_1 U^2. \tag{2.31}$$

3. Analytical formulation of the model problem

In order to examine the interaction of the coherent jet structure with the turbulent shear layer we first introduce a formal partition of the field variables characterized by

$$p(r, x, t) = \bar{p}(r, x, t) + p'(r, x, t) \tag{3.1}$$

In this equation, and in analogous expressions involving the other flow variables, the overbar denotes the coherent or mean component of the field which we now define precisely as the average with respect to an ensemble of realizations of the turbulent fluctuation ξ. Primed quantities represent the random fluctuations about the mean state and arise as a result of the interaction of the coherent jet structure and the turbulent shear layer. When the characteristic root mean square turbulent Mach number $\epsilon = \sqrt{\langle \xi^2 \rangle}/c_1$ is small, the interaction may be treated as a scattering problem. To do this it is convenient to adopt the stagnation enthalpy B of equation (2.22) as the fundamental perturbation variable.

Consider first conditions within the shear layer $a < r < b$. Viscosity and heat conduction are being neglected and the flow is therefore isentropic. The inhomogeneous wave equation which determines the stagnation enthalpy in terms of the other flow variables has the corresponding form

$$\frac{\mathrm{D}}{\mathrm{D}t}\left(\frac{1}{c_1^2}\frac{\mathrm{D}}{\mathrm{D}t}\right) B + \frac{1}{c_1^2}\frac{\mathrm{D}\boldsymbol{v}}{\mathrm{D}t}\cdot\nabla B - \nabla^2 B = \operatorname{div}(\boldsymbol{\omega}\wedge\boldsymbol{v}) - \frac{1}{c_1^2}\frac{\mathrm{D}\boldsymbol{v}}{\mathrm{D}t}\cdot(\boldsymbol{\omega}\wedge\boldsymbol{v}) \tag{3.2}$$

(Howe 1975). Here $\mathrm{D}/\mathrm{D}t = \partial/\partial t + \boldsymbol{v}\cdot\nabla$ is the material derivative.

The right hand side of equation (3.2) contains two distinct contributions. The first is proportional to the square of the small local perturbation velocity induced by the frozen, convected vorticity distribution (2.17) and will be discarded. It describes the generation of sound by the shear layer turbulence. The mean density is uniform within the shear layer and the vorticity of a fluid element is conserved, therefore the second contribution to the right of (3.2) comes from the

interaction of the vorticity $\boldsymbol{\omega}$ of (2.17) with the component of the perturbation velocity $\boldsymbol{v}$ produced by the pressure distribution (2.21) imposed on the boundary $r = b$ of the jet. This pressure distribution will henceforth be referred to as the 'incident wave'. For small turbulent fluctuation velocities the leading interaction product is provided by the first term on the right of equation (3.2).

Similarly, in the vicinity of the random vorticity layer, the final term on the left of (3.2) is the only one capable of accounting for the singular variation in B across the layer. The second term is $O(\epsilon^2)$ smaller, and the first is finite because of the material derivatives. Hence the variable coefficients of those terms may be discarded since they are negligible in other regions of the flow.

Taking account of all these remarks enables us to reduce equation (3.2) for the acoustic disturbance within the shear layer to the form

$$\left(\frac{1}{c_1^2}\frac{\partial^2}{\partial t^2} - \nabla^2\right) B = \operatorname{div}(\boldsymbol{\omega} \wedge \boldsymbol{v}), \tag{3.3}$$

where on the right-hand side $\boldsymbol{v}$ now denotes the component of the perturbation velocity due to the presence of the shock cells.

In this equation B and $\boldsymbol{v}$ may both be partitioned into coherent and random components as in equation (3.1). When equation (3.3) is averaged over an ensemble of realizations of the random vorticity field ξ we than have

$$\left(\frac{1}{c_1^2}\frac{\partial^2}{\partial t^2} - \nabla^2\right) \bar{B} = \operatorname{div}\langle \boldsymbol{\omega} \wedge \boldsymbol{v}' \rangle, \tag{3.4}$$

since $\langle \boldsymbol{\omega} \rangle \equiv \mathbf{0}$. This describes the evolution of the coherent field within the shear layer, the term on the right hand side accounting for the effect of turbulent diffusion. Subtracting (3.4) from the full equation (3.3) yields

$$\left(\frac{1}{c_1^2}\frac{\partial^2}{\partial t^2} - \nabla^2\right) B' = \operatorname{div}\{\boldsymbol{\omega} \wedge \boldsymbol{v} - \langle \boldsymbol{\omega} \wedge \boldsymbol{v}' \rangle\}, \tag{3.5}$$

which expresses the random fluctuations in the stagnation enthalpy in terms of the interaction of the shock-cell induced perturbation velocity with the turbulence.

In other regions of the flow the mean and random components of the wave field both satisfy the homogeneous convected wave equation. Within the jet core ($r < a$) this is

$$\left\{\frac{1}{c_1^2}\left(\frac{\partial}{\partial t} + [U - V]\frac{\partial}{\partial x}\right)^2 - \nabla^2\right\} B = 0; \tag{3.6}$$

and in the ambient medium ($r > b$) we have

$$\left\{\frac{1}{c_0^2}\left(\frac{\partial}{\partial t} - V\frac{\partial}{\partial x}\right)^2 - \nabla^2\right\} B = 0. \tag{3.7}$$

In all cases the perturbed flow is axisymmetric, and

$$\nabla^2 \equiv \frac{\partial^2}{\partial x^2} + \frac{1}{r}\frac{\partial}{\partial r}\left(r\frac{\partial}{\partial r}\right). \tag{3.8}$$

4. The coherent field equations

The incident pressure wave (2.21) may be cast in the following integral form:

$$\bar{p} = \iint_{-\infty}^{\infty} S(k, \omega)\, \mathrm{e}^{\mathrm{i}(kx-\omega t)}\, \mathrm{d}k\, \mathrm{d}\omega, \tag{4.1}$$

where

$$S = \frac{-P}{2\pi \mathrm{i} k}\, \delta(\omega + Vk). \tag{4.2}$$

It follows that, since in the x-reference frame the random vorticity distribution $\boldsymbol{\omega}$ does not depend on the time, the analysis of the interaction between the incident wave and the turbulent fluctuations may be simplified by first considering a single harmonic component proportional to $\exp(-\mathrm{i}\omega t)$, the complete result being obtained subsequently by integration with respect to the radian frequency ω. We shall suppress the explicit dependence on this time factor, and note that in equations (3.4)–(3.7) $\partial/\partial t \equiv -\mathrm{i}\omega$.

The discussion of these equations is further facilitated by Fourier transforming with respect to x, in accordance with the definition (2.3). In $a < r < b$ we then have:

$$\left.\begin{aligned} \left(\frac{1}{r}\frac{\partial}{\partial r}\left(r\frac{\partial}{\partial r}\right) + \Gamma^2\right)\hat{B} &= -\mathscr{F}_1, \\ \left(\frac{1}{r}\frac{\partial}{\partial r}\left(r\frac{\partial}{\partial r}\right) + \Gamma^2\right)\hat{B}' &= -\mathscr{F}_2, \end{aligned}\right\} \tag{4.3a, b}$$

where

$$\Gamma^2 \equiv \Gamma(k)^2 = \omega^2/c_1^2 - k^2, \tag{4.4}$$

and $\mathscr{F}_1$, $\mathscr{F}_2$ are the Fourier transforms of the 'source' terms defined by

$$\left.\begin{aligned} \mathscr{F}_1 &= \frac{1}{2\pi}\int_{-\infty}^{\infty} \mathrm{div}\langle \boldsymbol{\omega} \wedge \boldsymbol{v}' \rangle\, \mathrm{e}^{-\mathrm{i}kx}\, \mathrm{d}x, \\ \mathscr{F}_2 &= \frac{1}{2\pi}\int_{-\infty}^{\infty} \mathrm{div}\{\boldsymbol{\omega} \wedge \boldsymbol{v} - \langle \boldsymbol{\omega} \wedge \boldsymbol{v}' \rangle\}\, \mathrm{e}^{-\mathrm{i}kx}\, \mathrm{d}x. \end{aligned}\right\} \tag{4.5a, b}$$

Similarly, equations (3.6), (3.7) become

$$\left.\begin{aligned} \left(\frac{1}{r}\frac{\partial}{\partial r}\left(r\frac{\partial}{\partial r}\right) + \Gamma_{\mathrm{J}}^2\right)\hat{B} &= 0, \\ \left(\frac{1}{r}\frac{\partial}{\partial r}\left(r\frac{\partial}{\partial r}\right) + \gamma^2\right)\hat{B} &= 0, \end{aligned}\right\} \tag{4.6a, b}$$

where

$$\left.\begin{aligned} \Gamma_{\mathrm{J}}^2 &= [\omega - (U-V)\,k]^2/c_1^2 - k^2, \\ \gamma^2 &= (\omega + Vk)^2/c_0^2 - k^2. \end{aligned}\right\} \tag{4.7a, b}$$

Consider the coherent component of the wavefield. This must be a function of $(r, x+Vt)$ and each harmonic component of its Fourier transform will therefore be proportional to $\delta(\omega + Vk)$, as in (4.2). We may therefore assume at the outset that for the coherent field, ω, k satisfy

$$\omega + Vk = 0. \tag{4.8}$$

Also the coherent wave structure within the jet is at rest relative to the ambient medium, and in consequence $\bar{B}$ must vanish in $r > b$. The perturbed flow in the ambient medium therefore consists entirely of a random distribution of scattered disturbances.

By using (4.8) and the definitions (4.4), (4.7a) of Γ and Γ_J it follows that for the coherent component of the wavefield we may take

$$\Gamma = \beta_2 k, \quad \Gamma_J = \beta_1 k \tag{4.9}$$

where β_1 is defined in (2.5), and

$$\beta_2 = \sqrt{(V^2/c_1^2 - 1)} \tag{4.10}$$

a quantity which is pure imaginary if $V < c_1$.

Now the perturbed flow is axi-symmetric, so that taking account of the definition (2.17) of ω it is apparent that the transformed source term $\mathscr{F}_1$ of (4.5a) must have the form

$$\mathscr{F}_1 = \chi_1(k)\,\delta(r-h) + \chi_2(k)\,(h/r)\,\delta'(r-h), \tag{4.11}$$

where the prime denotes differentiation with respect to the argument. The *mean interaction functions* χ_1, χ_2 are $O(\epsilon^2)$ quantities and their explicit forms will be obtained in § 5.

Equations (4.3a), (4.6a) for the coherent field may now be solved formally by noting that the homogeneous equations are satisfied by zero order Bessel functions. In particular, in $a < r < b$ we may set

$$\begin{aligned}\hat{B} = {} & [\mathscr{A}_+ H_0^{(1)}(\beta_2 kr) + \mathscr{B}_+ H_0^{(2)}(\beta_2 kr)]\, H(r-h), \\ & + [\mathscr{A}_- H_0^{(1)}(\beta_2 kr) + \mathscr{B}_- H_0^{(2)}(\beta_2 kr)]\, H(h-r),\end{aligned} \tag{4.12}$$

where $H_0^{(1)}$, $H_0^{(2)}$ are Hankel functions of the first and second kind respectively, and $H(x)$ is the Heaviside unit function. This form takes account of the singular behaviour of $\hat{B}$ at $r = h$ resulting from the inhomogeneous term $\mathscr{F}_1$ on the right of (4.3a).

Within the inner jet flow ($0 \leqslant r < a$) the bounded solution of (4.6a) is

$$\hat{B} = \mathscr{D} J_0(\beta_1 kr). \tag{4.13}$$

The coefficients $\mathscr{A}_\pm$, $\mathscr{B}_\pm$ and $\mathscr{D}$ are related by the boundary conditions which must be satisfied at the mean positions $r = a$, $r = b$ of the interfaces. These are (i) continuity of pressure; (ii) continuity of fluid particle displacement normal to the interface.

On either side of an interface, and in regions of the flow not occupied by the vorticity fluctuations ω, the Bernoulli equation (2.25) indicates that we may take

$$B = -\partial\phi/\partial t \equiv \mathrm{i}\omega\phi, \tag{4.14}$$

where ϕ is the velocity potential. It follows in the usual way that

$$\left.\begin{aligned}\bar{p} &= \rho_1 \bar{B} \qquad (a < r < b), \\ &= \rho_1 (U/V)\,\bar{B} \quad (0 \leqslant r < a),\end{aligned}\right\} \tag{4.15}$$

and therefore that continuity of pressure at $r = a$ requires that

$$\mathscr{A}_- H_0^{(1)}(\beta_2 ka) + \mathscr{B}_- H_0^{(2)}(\beta_2 ka) = (U/V)\,\mathscr{D} J_0(\beta_1 ka). \tag{4.16}$$

At $r = b$ the pressure must equal that of the corresponding harmonic component of the incident wave (2.21), i.e. by using the transform representation (4.2)

$$\mathscr{A}_+ H_0^{(1)}(\beta_2 kb) + \mathscr{B}_+ H_0^{(2)}(\beta_2 kb) = S/\rho_1. \tag{4.17}$$

Continuity of fluid particle displacement implies also that

$$(\partial\bar{\phi}/\partial r)/(\omega - vk)$$

is continuous at the mean positions of the interfaces, where v is the local mean axial convection velocity. This condition need only be applied at $r = a$ since $\partial\overline{\phi}/\partial r$ vanishes identically in the ambient medium. In $a < r < b$, $v = 0$, and in $0 \leqslant r < a$, $v = U - V$ hence making use of (4.8) we have at $r = a$

$$(\beta_2/V)\{\mathscr{A}_- H_1^{(1)}(\beta_2 ka) + \mathscr{B}_- H_1^{(2)}(\beta_2 ka)\} = (\beta_1/U)\,\mathscr{D} J_1(\beta_1 ka). \tag{4.18}$$

It remains to write down the condition that the discontinuous expression (4.12) satisfies equation (4.3a). Substituting (4.12) into the left hand side of (4.3a) we obtain

$$\begin{aligned}&[(\mathscr{A}_+ - \mathscr{A}_-) H_0^{(1)}(\beta_2 kh) + (\mathscr{B}_+ - \mathscr{B}_-) H_0^{(2)}(\beta_2 kh)]\,(h/r)\,\delta'(r-h)\\ &\quad -[(\mathscr{A}_+ - \mathscr{A}_-) H_1^{(1)}(\beta_2 kh) + (\mathscr{B}_+ - \mathscr{B}_-) H_1^{(2)}(\beta_2 kh)]\,\beta_2 k\delta(r-h) = -\mathscr{F}_1.\end{aligned} \tag{4.19}$$

Using (4.11) and equating coefficients of $\delta(r-h)$, $\delta'(r-h)$ we find

$$\left.\begin{aligned}(\mathscr{A}_+ - \mathscr{A}_-) H_1^{(1)}(\beta_2 kh) + (\mathscr{B}_+ - \mathscr{B}_-) H_1^{(2)}(\beta_2 kh) &= \chi_1/\beta_2 k,\\ (\mathscr{A}_+ - \mathscr{A}_-) H_0^{(1)}(\beta_2 kh) + (\mathscr{B}_+ - \mathscr{B}_-) H_0^{(2)}(\beta_2 kh) &= -\chi_2.\end{aligned}\right\} \tag{4.20}$$

Equations (4.16)–(4.20) are sufficient to determine $\mathscr{A}_\pm$, $\mathscr{B}_\pm$, $\mathscr{D}$ in terms of the Fourier coefficient S of the incident pressure wave and the mean interaction functions χ_1, χ_2.

From (4.20), and making use of the Wronskian

$$H_1^{(1)}(z)\,H_0^{(2)}(z) - H_0^{(1)}(z)\,H_1^{(2)}(z) = -4\mathrm{i}/\pi z \tag{4.21}$$

(Abramowitz & Stegun 1965, p. 360), we may also write

$$\left.\begin{aligned}\mathscr{A}_+ &= \mathscr{A}_- + \tfrac{1}{4}\pi\mathrm{i}\beta_2 kh\{\chi_2 H_1^{(2)}(\beta_2 kh) + (\chi_1/\beta_2 k)\,H_0^{(2)}(\beta_2 kh)\},\\ \mathscr{B}_+ &= \mathscr{B}_- - \tfrac{1}{4}\pi\mathrm{i}\beta_2 kh\{\chi_2 H_1^{(1)}(\beta_2 kh) + (\chi_1/\beta_2 k)\,H_0^{(1)}(\beta_2 kh)\}.\end{aligned}\right\} \tag{4.22}$$

Using these results in (4.17) we obtain the following equation involving $\mathscr{A}_-$, $\mathscr{B}_-$ alone

$$\begin{aligned}&\mathscr{A}_- H_0^{(1)}(\beta_2 kb) + \mathscr{B}_- H_0^{(2)}(\beta_2 kb) + \tfrac{1}{4}\pi\mathrm{i}\beta_2 kh\chi_2[H_0^{(1)}(\beta_2 kb)\,H_1^{(2)}(\beta_2 kh) - H_0^{(2)}(\beta_2 kb)\,H_1^{(1)}(\beta_2 kh)]\\ &\quad + \tfrac{1}{4}\pi\mathrm{i}h\chi_1[H_0^{(1)}(\beta_2 kb)\,H_0^{(2)}(\beta_2 kh) - H_0^{(2)}(\beta_2 kb)\,H_0^{(1)}(\beta_2 kh)] = S/\rho_1.\end{aligned} \tag{4.23}$$

To proceed beyond this point requires a determination of the explicit forms of the mean interaction functions χ_1, χ_2. This is the subject of the next section.

5. The random field equations

The mean interaction functions χ_1, χ_2 of equation (4.11) depend on the random component $\boldsymbol{v}'$ of the acoustic velocity and on the vorticity $\boldsymbol{\omega}$ through the definition (4.5a) of $\mathscr{F}_1$. The velocity $\boldsymbol{v}'$ may be calculated once the corresponding component B' of the stagnation enthalpy has been determined.

Now B' satisfies equation (4.3b), where it appears both explicitly on the left-hand side and implicitly in terms of $\boldsymbol{v}'$ on the right by virtue of equation (4.5b) for $\mathscr{F}_2$. By setting

$$\boldsymbol{v} = \overline{\boldsymbol{v}} + \boldsymbol{v}', \tag{5.1}$$

equation (4.3b) becomes:

$$\begin{aligned}\left(\frac{1}{r}\frac{\partial}{\partial r}\left(r\frac{\partial}{\partial r}\right) + \Gamma^2\right)\hat{B}' &= -\frac{1}{2\pi}\int_{-\infty}^{\infty} \mathrm{div}\,(\boldsymbol{\omega}\wedge\overline{\boldsymbol{v}})\,\mathrm{e}^{-\mathrm{i}kx}\,\mathrm{d}x.\\ &\quad -\frac{1}{2\pi}\int_{-\infty}^{\infty} \mathrm{div}\,\{\boldsymbol{\omega}\wedge\boldsymbol{v}' - \langle\boldsymbol{\omega}\wedge\boldsymbol{v}'\rangle\}\,\mathrm{e}^{-\mathrm{i}kx}\,\mathrm{d}x.\end{aligned} \tag{5.2}$$

The first term on the right of (5.2) describes the interaction between the coherent velocity $\bar{\boldsymbol{v}}$ and the turbulent vorticity fluctuations $\boldsymbol{\omega}$, and is the effective source of the random wavefield. The second term on the right accounts for the subsequent multiple interactions of the random field with the flow inhomogeneities; their effect is cumulative and must be taken into account when it is desired to examine the propagation of the random field within the jet over many characteristic wavelengths. However, our present concern is with the determination of the Fourier transform $\mathscr{F}_1$ of the divergence of the mean interaction product

$$\langle \boldsymbol{\omega} \wedge \boldsymbol{v}' \rangle \equiv \langle \boldsymbol{\omega}(\boldsymbol{x}) \wedge \boldsymbol{v}'(\boldsymbol{x}, t) \rangle, \tag{5.3}$$

and it is apparent that only those contributions to $\boldsymbol{v}'$ which are correlated with the random vorticity fluctuations at $\boldsymbol{x}$ will make a non-trivial contribution to this mean value. In other words, only that part of the random acoustic field which has experienced an interaction with the turbulent flow within distances of the order of the turbulence correlation scale l, say, of the point $\boldsymbol{x}$ will be significant. For small values of the turbulent Mach number ϵ multiple scattering may be neglected over distances of order l, and in this case the leading contribution to the right hand side of (5.2) is furnished by the first term describing the coherent field interaction. The multiple scattering term on the right of (5.2) results in a contribution to the mean value of equation (5.3) which is at least $O(\epsilon)$ smaller.

Thus in estimating the mean interaction functions χ_1, χ_2 defined by $\mathscr{F}_1$ it is sufficient to adopt the *local Born approximation*

$$\left(\frac{1}{r}\frac{\partial}{\partial r}\left(r\frac{\partial}{\partial r}\right) + \Gamma^2\right)\hat{B}' = -\frac{1}{2\pi}\int_{-\infty}^{\infty} \operatorname{div}(\boldsymbol{\omega} \wedge \bar{\boldsymbol{v}})\, \mathrm{e}^{-\mathrm{i}kx}\, \mathrm{d}x, \tag{5.4}$$

provided that the fluctuation Mach number ϵ is small. This is equivalent to taking the following approximation to the random equation (3.5):

$$\left(\frac{1}{c_1^2}\frac{\partial^2}{\partial t^2} - \nabla^2\right) B' = \operatorname{div}(\boldsymbol{\omega} \wedge \bar{\boldsymbol{v}}). \tag{5.5}$$

It is a familiar procedure in problems of wave propagation in random media, and further discussion of its justification may be found in Frisch (1968) and Howe (1971, 1973).

Equation (5.4) may now be solved in conjunction with equations (4.6) and the radiation condition that in the ambient medium all random disturbances are generated within the jet flow. In doing this we neglect the diffraction of the scattered field by the nozzle, an approximation which is not expected to affect the main conclusions of the analysis. The procedure is similar to that already outlined in the previous section in connection with the coherent field, and only the principal steps will be described here.

Let $(\bar{u}, \bar{v})$ denote the (x, r) coherent field components of $\bar{\boldsymbol{v}}$ on the surface $r = h$ occupied by the random vorticity fluctuations. Then

$$\boldsymbol{\omega} \wedge \bar{\boldsymbol{v}} = (-\bar{v}, \bar{u})\, \xi(x)\, \delta(r-h), \tag{5.6}$$

and (5.4) becomes:

$$\left(\frac{1}{r}\frac{\partial}{\partial r}\left(r\frac{\partial}{\partial r}\right) + \Gamma^2\right)\hat{B}' = \frac{1}{2\pi}\int_{-\infty}^{\infty}\left\{\mathrm{i}K\bar{v}(X)\,\delta(r-h) - \frac{h}{r}\bar{u}(X)\,\delta'(r-h)\right\}\xi(X)\,\mathrm{e}^{-\mathrm{i}KX}\,\mathrm{d}X, \tag{5.7}$$

where here and henceforth in dealing with the Fourier representation of the wavefield it is convenient to use capital K for the wavenumber of the random field and to reserve the lower case k for the coherent field.

A particular integral $\hat{B}'_{\mathrm{p}}$ of (5.7) may be set in the form

$$\hat{B}'_{\mathrm{p}} = B'_{+} H_0^{(1)}(\Gamma r) H(r-h) + B'_{-} H_0^{(2)}(\Gamma r) H(h-r) \tag{5.8}$$

for $a < r < b$. The coefficients $B'_{\pm}$ are determined by substituting into (5.7) and equating the coefficients of $\delta(r-h)$, $\delta'(r-h)$. The complete representation of the random field is then obtained by augmenting (5.8) with solutions of the homogeneous equations (5.6), (4.6) and applying the conditions of continuity of pressure and fluid particle displacement at the mean positions $r = a, b$ of the interfaces.

In executing this procedure it is convenient to use the velocity potential ϕ' rather than B'. In the ambient medium $r > b$, the appropriate solution of (4.6b) is then

$$\hat{\phi}' = T H_0^{(1)}(\gamma r), \tag{5.9}$$

where T is to be determined, and the radiation condition is satisfied by taking that branch of $\gamma(K)$ which is defined for real values of the wavenumber K by

$$\gamma(K) = \begin{cases} \operatorname{sgn}(\omega + VK) \\ +\mathrm{i} \end{cases} \left| \frac{(\omega + VK)^2}{c_0^2} - K^2 \right|^{\frac{1}{2}}, \tag{5.10}$$

according as $(\omega + VK)^2/c_0^2 \gtrless K^2$. This condition is equivalent to assigning to the radian frequency ω a small positive imaginary component (Lighthill 1960). When $\gamma(K)$ is taken to be positive imaginary for $(\omega + VK)^2/c_0^2 < K^2$, its value for all real K is automatically fixed since the branch points of the square root are now displaced infinitesimally from the real axis.

Within the shear layer $(a < r < b)$:

$$\left.\begin{aligned} \hat{\phi}' &= (B^{(2)} + C) H_0^{(1)}(\Gamma r) + A H_0^{(2)}(\Gamma r) \quad (r > h), \\ &= C H_0^{(1)}(\Gamma r) + (B^{(1)} + A) H_0^{(2)}(\Gamma r) \quad (r < h), \end{aligned}\right\} \tag{5.11}$$

the coefficients A, C are to be found, and the $B^{(i)}$ correspond to the particular integral (5.7) of the inhomogeneous equation (5.6) discussed above, and have the explicit representation

$$B^{(i)} = (h/8\omega) \int_{-\infty}^{\infty} \{\Gamma \bar{u}(X) H_1^{(i)}(\Gamma h) - \mathrm{i} K \bar{v}(X) H_0^{(i)}(\Gamma h)\} \xi(X) \, \mathrm{e}^{-\mathrm{i}KX} \, \mathrm{d}X, \tag{5.12}$$

$(i = 1, 2)$, with $\Gamma \equiv \Gamma(K)$.

Within the inner jet flow $(r < a)$ the 'random' potential is

$$\hat{\phi}' = D J_0(\Gamma_{\mathrm{J}} r), \tag{5.13}$$

where $\Gamma_{\mathrm{J}} \equiv \Gamma_{\mathrm{J}}(K)$.

Applying the conditions of continuity of pressure at the mean positions $r = a, b$ of the interfaces, we have

$$\left.\begin{aligned} (B^{(1)} + A) H_0^{(2)}(\Gamma a) + C H_0^{(1)}(\Gamma a) &= \left(\frac{\omega - (U-V)K}{\omega}\right) D J_0(\Gamma_{\mathrm{J}} a), \\ A H_0^{(2)}(\Gamma b) + (B^{(2)} + C) H_0^{(1)}(\Gamma b) &= \left(\frac{\omega + VK}{\omega}\right) \frac{\rho_0}{\rho_1} T H_0^{(1)}(\gamma b). \end{aligned}\right\} \tag{5.14}$$

Similarly, continuity of fluid particle displacement gives

$$\left.\begin{aligned} (B^{(1)} + A) H_1^{(2)}(\Gamma a) + C H_1^{(1)}(\Gamma a) &= \left(\frac{\omega}{\omega - (U-V)K}\right) \frac{\Gamma_{\mathrm{J}}}{\Gamma} D J_1(\Gamma_{\mathrm{J}} a), \\ A H_1^{(2)}(\Gamma b) + (B^{(2)} + C) H_1^{(1)}(\Gamma b) &= \left(\frac{\omega}{\omega + VK}\right) \frac{\gamma}{\Gamma} T H_1^{(1)}(\gamma b). \end{aligned}\right\} \tag{5.15}$$

To calculate the random perturbation velocity $\boldsymbol{v}'$ at points within the shear layer, the system (5.14), (5.15) must be solved for the coefficients A, C. Introduce the following shorthand notation:

$$\left.\begin{aligned}\mu_0 &= \frac{\Gamma_J}{\Gamma}\left(\frac{\omega}{\omega-(U-V)K}\right)^2 \frac{J_1(\Gamma_J a)\,H_0^{(1)}(\Gamma a)}{J_0(\Gamma_J a)\,H_1^{(1)}(\Gamma a)},\\ \mu_1 &= \mu_0\frac{H_0^{(2)}(\Gamma a)}{H_0^{(1)}(\Gamma a)} - \frac{H_1^{(2)}(\Gamma a)}{H_1^{(1)}(\Gamma a)},\\ \mathscr{R}_1 &= (1-\mu_0)/\mu_1\end{aligned}\right\} \tag{5.16}$$

and

$$\left.\begin{aligned}\nu_0 &= \frac{\rho_1\gamma}{\rho_0\Gamma}\left(\frac{\omega}{\omega+VK}\right)^2 \frac{H_1^{(1)}(\gamma b)\,H_0^{(1)}(\Gamma b)}{H_0^{(1)}(\gamma b)\,H_1^{(1)}(\Gamma b)},\\ \nu_1 &= \nu_0\frac{H_0^{(2)}(\Gamma b)}{H_0^{(1)}(\Gamma b)} - \frac{H_1^{(2)}(\Gamma b)}{H_1^{(1)}(\Gamma b)},\\ \mathscr{R}_2 &= (1-\nu_0)/\nu_1.\end{aligned}\right\} \tag{5.17}$$

Then it is readily deduced that

$$A = \mathscr{R}_2(B^{(2)}+C); \quad A+B^{(1)} = \mathscr{R}_1 C, \tag{5.18}$$

and that

$$\left.\begin{aligned}A &= \frac{\mathscr{R}_2(B^{(1)}+\mathscr{R}_1 B^{(2)})}{\mathscr{R}_1-\mathscr{R}_2},\\ C &= \frac{B^{(1)}+\mathscr{R}_2 B^{(2)}}{\mathscr{R}_1-\mathscr{R}_2}.\end{aligned}\right\} \tag{5.19}$$

We are now ready to calculate the random velocity $\boldsymbol{v}'$ at the turbulent vorticity layer. Take the inverse Fourier transform of (5.11):

$$\left.\begin{aligned}\varphi' &= \int_{-\infty}^{\infty}\{(B^{(2)}+C)\,H_0^{(1)}(\Gamma r)+AH_0^{(2)}(\Gamma r)\}\,\mathrm{e}^{\mathrm{i}Kx}\,\mathrm{d}K \quad (h<r<b),\\ \varphi' &= \int_{-\infty}^{\infty}\{CH_0^{(1)}(\Gamma r)+(B^{(1)}+A)\,H_0^{(2)}(\Gamma r)\}\,\mathrm{e}^{\mathrm{i}Kx}\,\mathrm{d}K \quad (a<r<h).\end{aligned}\right\} \tag{5.20a, b}$$

These expressions indicate that φ' and its derivatives are discontinuous at $\Gamma = h$, which must be the case in order to account for the inhomogeneous term on the right of equation (5.4). However, the resulting discontinuity in the flow velocity at $r = h$ corresponds to the singularity which arises at an isolated line vortex in the flow induced by that vortex. The self-induced velocities are equal and opposite on either side of the vorticity layer, so that the actual value of $\boldsymbol{v}'$ at $r = h$ is given by the mean of the velocities predicted by (5.20a), (5.20b). Thus at the vorticity layer we have:

$$\begin{aligned}\boldsymbol{v}' = \frac{1}{2}\int_{-\infty}^{\infty}&(B^{(2)}+C)\,(\mathrm{i}K[H_0^{(1)}(\Gamma h)+\mathscr{R}_2 H_0^{(2)}(\Gamma h)],\ -\Gamma[H_1^{(1)}(\Gamma h)+\mathscr{R}_2 H_1^{(2)}(\Gamma h)])\,\mathrm{e}^{\mathrm{i}Kx}\mathrm{d}K\\ +\frac{1}{2}\int_{-\infty}^{\infty}&C(\mathrm{i}K[H_0^{(1)}(\Gamma h)+\mathscr{R}_1 H_0^{(2)}(\Gamma h)],\ -\Gamma[H_1^{(1)}(\Gamma h)+\mathscr{R}_1 H_1^{(2)}(\Gamma h)])\,\mathrm{e}^{\mathrm{i}Kx}\,\mathrm{d}K,\end{aligned} \tag{5.21}$$

where use has been made of (5.18).

Hence referring to the definition (2.17) of the turbulent vorticity $\boldsymbol{\omega}$, it follows that

$$\begin{aligned}\mathscr{F}_1 &= \frac{1}{2\pi}\int_{-\infty}^{\infty} \operatorname{div}\langle \boldsymbol{\omega}\wedge\boldsymbol{v}'\rangle \,\mathrm{e}^{-\mathrm{i}kx}\,\mathrm{d}x \\ &\equiv \chi_1\,\delta(r-h)+(\chi_2\,h/r)\,\delta'(r-h) \\ &= \frac{\mathrm{i}}{4\pi}\iint_{-\infty}^{\infty}\langle (B^{(2)}+C)\,\xi(x)\rangle\Big\{k\Gamma[H_1^{(1)}(\Gamma h)+\mathscr{R}_2 H_1^{(2)}(\Gamma h)]\,\delta(r-h) \\ &\quad +\frac{Kh}{\Gamma}[H_0^{(1)}(\Gamma h)+\mathscr{R}_2 H_0^{(2)}(\Gamma h)]\,\delta'(r-h)\Big\}\,\mathrm{e}^{-\mathrm{i}(k-K)x}\,\mathrm{d}K\,\mathrm{d}x \\ &\quad +\frac{\mathrm{i}}{4\pi}\iint_{-\infty}^{\infty}\langle C\xi(x)\rangle\Big\{k\Gamma[H_1^{(1)}(\Gamma h)+\mathscr{R}_1 H_1^{(2)}(\Gamma h)]\,\delta(r-h) \\ &\quad +\frac{Kh}{r}[H_0^{(1)}(\Gamma h)+\mathscr{R}_1 H_0^{(2)}(\Gamma h)]\,\delta'(r-h)\Big\}\,\mathrm{e}^{-\mathrm{i}(k-K)x}\,\mathrm{d}K\,\mathrm{d}x, \qquad (5.22)\end{aligned}$$

where $\Gamma\equiv\Gamma(K)$.

Consider the integration with respect to x in the second of the integral expressions on the right of this result, namely,

$$I=\int_{-\infty}^{\infty}\langle C\xi(x)\rangle\,\mathrm{e}^{-\mathrm{i}(k-K)x}\,\mathrm{d}x. \qquad (5.23)$$

From (5.12), (5.19) we can write

$$\begin{aligned}I=\frac{h}{8\omega(\mathscr{R}_1-\mathscr{R}_2)}\iint_{-\infty}^{\infty}&\langle\xi(x)\,\xi(X)\rangle\{\Gamma\bar{u}(X)[H_1^{(1)}(\Gamma h)+\mathscr{R}_2 H_1^{(2)}(\Gamma h)] \\ &-\mathrm{i}K\bar{v}(X)[H_0^{(1)}(\Gamma h)+\mathscr{R}_2 H_0^{(2)}(\Gamma h)]\}\exp(-\mathrm{i}[(k-K)x+KX])\,\mathrm{d}x\,\mathrm{d}X. \qquad (5.24)\end{aligned}$$

Using the definition (2.19) of the autocorrelation function $R(x)$ of $\xi(x)$, and setting $z=x-X$ we have

$$\begin{aligned}I=\frac{h}{8\omega(\mathscr{R}_1-\mathscr{R}_2)}\iint_{-\infty}^{\infty}&R(z)\{\Gamma\bar{u}(X)[H_1^{(1)}(\Gamma h)+\mathscr{R}_2 H_1^{(2)}(\Gamma h)] \\ &-\mathrm{i}K\bar{v}(X)[H_0^{(1)}(\Gamma h)+\mathscr{R}_2 H_0^{(2)}(\Gamma h)]\}\exp(-\mathrm{i}[(k-K)z+kX])\,\mathrm{d}z\,\mathrm{d}X, \qquad (5.25)\end{aligned}$$

i.e.,

$$I=\frac{\pi^2 h}{2\omega(\mathscr{R}_1-\mathscr{R}_2)}\Phi(k-K)\{\Gamma\hat{u}(k)[H_1^{(1)}(\Gamma h)+\mathscr{R}_2 H_1^{(2)}(\Gamma h)]-\mathrm{i}K\hat{v}(k)\,[H_0^{(1)}(\Gamma h)+\mathscr{R}_2 H_0^{(2)}(\Gamma h)]\}, \qquad (5.26)$$

where $\Gamma\equiv\Gamma(K)$, $\Phi(k)$ is the turbulence spectrum given by (2.20), and $(\hat{u}(k),\hat{v}(k))$ is the Fourier transform of the coherent velocity on $r=h$.

Hence inserting (5.26) into the second integral on the right of (5.22) together with an analogous result for the first integral, we finally deduce that

$$\chi_1(k)=\frac{\mathrm{i}\pi hk}{8\omega}\int_{-\infty}^{\infty}\frac{\Gamma\Phi(k-K)}{(\mathscr{R}_1-\mathscr{R}_2)}\{2\Gamma\hat{u}(k)f_1(K)-\mathrm{i}K\hat{v}(k)\,g(K)\}\,\mathrm{d}K, \qquad (5.27)$$

and

$$\chi_2(k)=\frac{\mathrm{i}\pi h}{8\omega}\int_{-\infty}^{\infty}\frac{K\Phi(k-K)}{(\mathscr{R}_1-\mathscr{R}_2)}\{\Gamma\hat{u}(k)\,g(K)-2\mathrm{i}K\hat{v}(k)f_0(K)\}\,\mathrm{d}K, \qquad (5.28)$$

where

$$f_i(K)=[H_i^{(1)}(\Gamma h)+\mathscr{R}_1 H_i^{(2)}(\Gamma h)]\,[H_i^{(1)}(\Gamma h)+\mathscr{R}_2 H_i^{(2)}(\Gamma h)] \qquad (5.29)$$

$(i=0,1)$ and,

$$\begin{aligned}g(K)=&[H_0^{(1)}(\Gamma h)+\mathscr{R}_1 H_0^{(2)}(\Gamma h)]\,[H_1^{(1)}(\Gamma h)+\mathscr{R}_2 H_1^{(2)}(\Gamma h)] \\ &+[H_0^{(1)}(\Gamma h)+\mathscr{R}_2 H_0^{(2)}(\Gamma h)]\,[H_1^{(1)}(\Gamma h)+\mathscr{R}_1 H_1^{(2)}(\Gamma h)]. \qquad (5.30)\end{aligned}$$

These results determine the desired explicit forms for the mean interaction functions χ_1, χ_2 which occur in equation (4.23).

6. The decay of the coherent structure of the jet

The results of §§ 4, 5 may now be used to calculate the coherent cell structure of the imperfectly expanded jet in the presence of the turbulent shear layer (2.17). The expressions (5.27), (5.28) for the mean interaction functions $\chi_1(k)$, $\chi_2(k)$ are substituted into equation (4.23). This is used together with equations (4.16), (4.18) to determine the coefficients $\mathscr{A}_-$, $\mathscr{B}_-$ and $\mathscr{D}$ of the coherent field. In doing this it is also necessary to express $(\hat{u}(k), \hat{v}(k))$, the coherent field velocity at $r = h$, and which occurs in (5.27), (5.28), explicitly in terms of these coefficients. Since χ_1, χ_2 are already quantities of $O(\epsilon^2)$ we may neglect the $O(\epsilon^2)$ discontinuity in the coherent field variables at $r = h$ in calculating $(\hat{u}(k), \hat{v}(k))$.

Thus the using relation

$$\hat{\phi} = -(\mathrm{i}/\omega)\hat{B} \tag{6.1}$$

we may assume from (4.12) that

$$\hat{\phi} = -(\mathrm{i}/\omega)\{\mathscr{A}_- H_0^{(1)}(\beta_2 kr) + \mathscr{B}_- H_0^{(2)}(\beta_2 kr)\} \tag{6.2}$$

in calculating $(\hat{u}(k), \hat{v}(k))$ for use in (5.27), (5.28). This gives:

$$\left.\begin{aligned} \hat{u} &= (k/\omega)\{\mathscr{A}_- H_0^{(1)}(\beta_2 kh) + \mathscr{B}_- H_0^{(2)}(\beta_2 kh)\}, \\ \hat{v} &= (\mathrm{i}\beta_2 k/\omega)\{\mathscr{A}_- H_1^{(1)}(\beta_2 kh) + \mathscr{B}_- H_1^{(2)}(\beta_2 kh)\}. \end{aligned}\right\} \tag{6.3}$$

It is difficult to perform the analytical programme outlined above in its full generality because of the complexity of the expressions involved. The difficulty arises because of the finite shear layer width $\delta = b - a$, giving rise to Bessel functions whose arguments depend on a, b and h and leading to complicated expressions which are not easily interpreted. We shall therefore assume that δ is small and specifically that for all coherent field wavenumbers k of interest

$$k\delta \ll 1. \tag{6.4}$$

This is equivalent to assuming that $\delta/a \ll 1$.

The details of the analysis will be described in the limit as $\delta \to 0$. The modifications required for small but finite values of $k\delta$ will be sketched-in subsequently in § 9.

The limiting case in which δ is allowed to vanish will still retain the essential physical qualities of the turbulence interaction problem provided that at least one of the mean interaction functions $\chi_1(k)$, $\chi_2(k)$ which account for the irreversible effects of turbulent diffusion continues to make a finite contribution. In fact, as $\delta \to 0$, the coefficient of χ_1 in (4.23) vanishes, but that of χ_2 tends to a finite limit, and (4.23) reduces to

$$\mathscr{A}_- H_0^{(1)}(\beta_2 ka) + \mathscr{B}_- H_0^{(2)}(\beta_2 ka) - \chi_2 = S/\rho_1. \tag{6.5}$$

The physical significance of this approximation will be discussed in § 8.

By using equation (4.16) this result may be expressed in the alternative form

$$(U/V)\mathscr{D}J_0(\beta_1 ka) - \chi_2 = S/\rho_1, \tag{6.6}$$

$\mathscr{D}$ being the Fourier coefficient defining the coherent field within the inner jet flow ($r < a$). Here χ_2 is an $O(\epsilon^2)$ quantity depending on the interaction between the random vorticity field $\boldsymbol{\omega}$ and the random wavefield $\boldsymbol{v}'$. When χ_2 is neglected, (6.6) determines the coefficient $\mathscr{D} \equiv \mathscr{D}(k)$ explicitly in terms of S, the Fourier transform of the incident pressure wave (2.21), and thereby leads directly to the representation (2.8) say, of the coherent field in the absence of turbulent diffusion.

Now in the limit as $\delta \to 0$, equations (4.16), (4.18) imply that (6.3) assumes the simplified form

$$\left.\begin{aligned} \hat{u}(k) &= (Uk/V\omega)\,\mathscr{D}J_0(\beta_1 ka), \\ \hat{v}(k) &= (\mathrm{i}\beta_1 Vk/U\omega)\,\mathscr{D}J_1(\beta_1 ka). \end{aligned}\right\} \tag{6.7}$$

Also it follows from (5.28) that as $\delta \to 0$

$$\chi_2(k) = \frac{1}{2\omega}\int \frac{K\Phi(k-K)}{\Gamma(\nu-\mu)}\{\Gamma(\nu+\mu)\,\hat{u}(k) - 2\mathrm{i}K\hat{v}(k)\}\,\mathrm{d}K, \tag{6.8}$$

where

$$\left.\begin{aligned} \mu &= \frac{\Gamma_J}{\Gamma}\left(\frac{\omega}{\omega-(U-V)K}\right)^2 \frac{J_1(\Gamma_J a)}{J_0(\Gamma_J a)}, \\ \nu &= \frac{\rho_0\gamma}{\rho_0\Gamma}\left(\frac{\omega}{\omega+VK}\right)^2 \frac{H_1^{(1)}(\gamma a)}{H_0^{(1)}(\gamma a)} \end{aligned}\right\} \tag{6.9}$$

and γ, Γ, Γ_J are functions of ω and K.

Hence substituting from (6.7) into (6.8) and inserting the resulting expression for χ_2 into equation (6.6) we obtain

$$\mathscr{D}(k)\left\{J_0(\beta_1 ka)\left[1 - \frac{k}{2\omega^2}\int_{-\infty}^{\infty} \frac{K\Gamma(\nu+\mu)}{(\nu-\mu)}\Phi(k-K)\,\mathrm{d}K\right] - J_1(\beta_1 ka)\,\beta_1\left(\frac{V}{U}\right)^2 \frac{k}{\omega^2}\int_{-\infty}^{\infty} \frac{K^2\Phi(k-K)\,\mathrm{d}K}{\Gamma(\nu-\mu)}\right\} = \frac{VS}{U\rho_1}. \tag{6.10}$$

This determines the Fourier coefficient $\mathscr{D}(k)$ defining the coherent field within the inner jet flow ($r < a$). Both of the integrals in the curly brackets of this equation are $O(\epsilon^2)$, and when ϵ is set equal to zero (6.10) becomes

$$\mathscr{D}(k) = \frac{VS}{\rho_1 UJ_0(\beta_1 ka)} \equiv \frac{-VP}{2\pi\mathrm{i}\rho_1 U}\frac{\delta(\omega+Vk)}{kJ_0(\beta_1 ka)}. \tag{6.11}$$

The properties of the coherent field are determined by the poles of $\mathscr{D}(k)$ in the k-plane. When ϵ vanishes these lie on the real axis at $k = 0$ and at the zeros of $J_0(\beta_1 ka)$, as in § 2. When $\epsilon \neq 0$ the effect of turbulent diffusion is to displace the poles other than that at $k = 0$ from the real axis. To determine their new locations observe that correct to $O(\epsilon^2)$ equation (6.10) becomes

$$\mathscr{D}(k) = \frac{(VS/\rho_1 U)}{\left[1 - \frac{k}{2\omega^2}\int_{-\infty}^{\infty} \frac{K\Gamma(\nu+\mu)}{(\nu-\mu)}\Phi(k-K)\,\mathrm{d}K\right]\left[J_0(\beta_1 ka) - J_1(\beta_1 ka)\frac{\beta_1 V^2 k}{U^2\omega^2}\int_{-\infty}^{\infty} \frac{K^2\Phi(k-K)}{\Gamma(\nu-\mu)}\mathrm{d}K\right]}. \tag{6.12}$$

Since ϵ is small the first factor in the denominator on the right may be replaced by unity. The poles of $\mathscr{D}(k)$ are given by the zeros of the factor involving the Bessel functions, and for small values of ϵ these zeros are close to those of $J_0(\beta_1 ka)$. The real part of the integral in this factor gives the $O(\epsilon^2)$ displacement of the root along the real axis, and will be ignored. Thus, defining the *dissipation function*, $\Delta_0(k)$, by

$$\Delta_0(k) = \mathrm{Im}\left\{-\frac{\beta_1 V^2 k}{U^2\omega^2}\int_{-\infty}^{\infty} \frac{K^2\Phi(k-K)}{\Gamma(\nu-\mu)}\mathrm{d}K\right\}, \tag{6.13}$$

we deduce that in the present approximation (6.12) is just

$$\mathscr{D}(k) = \frac{(VS/\rho_1 U)}{\{J_0(\beta_1 ka) + \mathrm{i}\Delta_0(k)\,J_1(\beta_1 ka)\}}. \tag{6.14}$$

But to $O(\epsilon^2)$ we may write

$$J_0(\beta_1 ka) + \mathrm{i}\Delta_0(k)\, J_1(\beta_1 ka) = J_0(\beta_1 ka - \mathrm{i}\Delta_0(k)), \tag{6.15}$$

in which case (6.14) becomes $$\mathscr{D}(k) = \frac{VS}{\rho_1 U J_0(\beta_1 ka - \mathrm{i}\Delta_0(k))}. \tag{6.16}$$

Observe that for the coherent structure of the jet to decay with distance downstream of the nozzle, the poles of $\mathscr{D}(k)$ must actually be displaced into the *upper* half of the k-plane, i.e. we must have $\Delta_0(k) > 0$.

Using (4.2) we may also write

$$\mathscr{D}(k) = \frac{-VP\delta(\omega + Vk)}{2\pi\mathrm{i}\rho_1 UkJ_0(\beta_1 ka - \mathrm{i}\Delta_0(k))}. \tag{6.17}$$

Substituting into equation (4.13), taking the inverse Fourier transform and performing the integration over all radian frequencies ω, finally yields the following expression for the coherent field

within the jet $(r < a)$ $$\bar{B} = \frac{-VP}{2\pi\mathrm{i}\rho_1 U}\int_{-\infty}^{\infty} \frac{J_0(\beta_1 kr)\, \mathrm{e}^{\mathrm{i}k(x+Vt)}}{(k - \mathrm{i}\sigma)\, J_0(\beta_1 ka - \mathrm{i}\Delta_0(k))}\, \mathrm{d}k. \tag{6.18}$$

The corresponding integral representation of the coherent pressure distribution within the jet may also be written down, and takes the form (2.13) foreshadowed in our preliminary discussion of the general problem.

7. Physical interpretation of the dissipation function $\Delta_0(k)$

The theoretical model developed above to account for the decay of the coherent structure of the imperfectly expanded jet is based on scattering theory in which the energy in the coherent wave system is redistributed over a spectrum of scattered disturbances. The scattered field consists of a continuum of sound waves which radiate away from the jet into the ambient medium, together with a discrete spectrum of trapped waves propagating parallel to the jet axis and decaying exponentially with radial distance in free space. Let us now derive an analytical representation of this result in terms of the dissipation function $\Delta_0(k)$.

Note first of all that, from (6.9)

$$\Gamma(\nu - \mu) = \frac{\rho_1 \gamma}{\rho_0}\left(\frac{\omega}{\omega + VK}\right)^2 \frac{H_1^{(1)}(\gamma a)}{H_0^{(1)}(\gamma a)} - \Gamma_{\mathrm{J}}\left(\frac{\omega}{\omega - (U-V)K}\right)^2 \frac{J_1(\Gamma_{\mathrm{J}} a)}{J_0(\Gamma_{\mathrm{J}} a)}. \tag{7.1}$$

This is a function of ω, K and its zeros define the eigenmodes of a circular cylindrical jet of radius a (see, for example, Morgan 1975). Those zeros which correspond to trapped modes within the jet lie on the real K-axis when the radian frequency ω is real, and the integral in (6.13) for the dissipation function $\Delta_0(k)$ is undefined until the manner in which the contour of integration negotiates the singularities of the denominator is prescribed. It has been noted in §5, however, that the radiation condition may be fulfilled by assigning to ω a small positive imaginary component, i.e. replacing ω by $\omega + \mathrm{i}\sigma$ $(\sigma > 0)$, say. The effect is to shift the singularities from the real axis and thereby remove the apparent indeterminateness in the value of the integral (6.13).

Since the turbulence spectrum $\Phi(k - K)$ is real when k, K are real it follows that (6.13) may be expressed in the equivalent form

$$\Delta_0(k) = -\frac{\beta_1 V^2 k}{2\mathrm{i}U^2\omega^2}\int_{-\infty}^{\infty} K^2\Phi(k-K)\left\{\frac{1}{\Gamma(\nu-\mu)} - \text{c.c.}\right\}\mathrm{d}K. \tag{7.2}$$

Set
$$Q(k,K) = 1/\Gamma(\nu-\mu) - \text{c.c.} \tag{7.3}$$
This is pure imaginary. As $\sigma \to +0$ two cases arise depending on the limiting value of $\Gamma(\nu-\mu)$.

Suppose first that $\Gamma(\nu-\mu) \neq 0$ as $\sigma \to +0$. From (7.1) it is clear that because Γ_J is either real or pure imaginary for real values of K, the second term on the right of (7.1) is always real (Abramowitz & Stegun 1965, p. 375). The first term, involving the Hankel functions, is real provided that $\gamma \equiv \gamma(\omega, K)$ is pure imaginary (cf. equation (5.10)), and when this is so $Q(k,K)$ vanishes identically. For those values of K for which γ is *real*, (7.3) becomes
$$Q(k,K) = \frac{(\rho_1/\rho_0)}{|\Gamma|^2|\nu-\mu|^2|H_0^{(1)}(\gamma a)|^2}\left(\frac{\omega}{\omega+VK}\right)^2 \times \{\gamma^* H_1^{(1)}(\gamma a)^* H_0^{(1)}(\gamma a) - \gamma H_1^{(1)}(\gamma a)\, H_0^{(1)}(\gamma a)^*\}, \tag{7.4}$$
where the asterisk denotes the complex conjugate of a function and for which $\omega + \mathrm{i}\sigma$ is replaced by $\omega - \mathrm{i}\sigma$. Using standard results listed in Abramowitz & Stegun (1965, pp. 360, 361), we then find that as $\sigma \to +0$
$$Q(k,K) = \frac{4\mathrm{i}\,\mathrm{sgn}\,(\gamma)\,(\rho_1/\rho_0)}{\pi a|\Gamma|^2|\nu-\mu|^2|H_0^{(1)}(\gamma a)|^2}\left(\frac{\omega}{\omega+VK}\right)^2, \tag{7.5}$$
for real γ.

Next suppose that $\Gamma(\nu-\mu) = 0$ as $\sigma \to +0$. This occurs for real values of k, K when γ is pure imaginary and both terms on the right of (7.1) are real. Let $K = K_n$ define the location of a real zero of
$$F(\omega, K) \equiv \Gamma(\nu-\mu). \tag{7.6}$$
For $K \simeq K_n$ we have
$$F(\omega+\mathrm{i}\sigma, K) \simeq (K-K_n)\,(\partial F/\partial K)_n + \mathrm{i}\sigma(\partial F/\partial\omega)_n, \tag{7.7}$$
where the partial derivatives are evaluated at (ω, K_n). Hence near $K = K_n$,
$$\begin{aligned} Q(k,K) &= \frac{1}{F(\omega+\mathrm{i}\sigma,K)} - \frac{1}{F(\omega-\mathrm{i}\sigma,K)} \\ &\approx \frac{-2\mathrm{i}\sigma\left(\dfrac{\partial F}{\partial\omega}\Big/\dfrac{\partial F}{\partial K}\right)_n}{\left(\dfrac{\partial F}{\partial K}\right)_n\left\{(K-K_n)^2 + \sigma^2\left(\dfrac{\partial F}{\partial\omega}\Big/\dfrac{\partial F}{\partial K}\right)_n^2\right\}} \\ &\to -\frac{2\pi\mathrm{i}\,\mathrm{sgn}\,(\partial F/\partial\omega)_n}{|(\partial F/\partial K)_n|}\,\delta(K-K_n) \end{aligned} \tag{7.8}$$
as $\sigma \to +0$. Taking account of all possible values of K_n, this result may be expressed in the more compact form:
$$Q(k,K) = -2\pi\mathrm{i}\,\mathrm{sgn}\,(\partial F/\partial\omega)\,\delta\{F(\omega,K)\}, \tag{7.9}$$
where K is restricted to those real values for which $F(\omega,K) \equiv \Gamma(\nu-\mu)$ is real.

Combining the results (7.5), (7.9) the representation (7.2) becomes
$$\begin{aligned} \Delta_0(k) = &-\frac{2\beta_1 V^2\rho_1 k}{\pi a U^2\rho_0\omega^2}\int^{\mathrm{Re}\,(\gamma)} \frac{\mathrm{sgn}\,(\gamma)\,K^2\Phi(k-K)}{|\Gamma|^2|\nu-\mu|^2|H_0^{(1)}(\gamma a)|^2}\left(\frac{\omega}{\omega+VK}\right)^2 \mathrm{d}K. \\ &+\frac{\pi\beta_1 V^2 k}{U^2\omega^2}\int^{\mathrm{Im}\,(\gamma)} \mathrm{sgn}\,(\partial F/\partial\omega)\,K^2\,\Phi(k-K)\,\delta\{F(\omega,K)\}\,\mathrm{d}K, \end{aligned} \tag{7.10}$$
in which the notation Re (γ), Im (γ) indicates respectively that the integration is restricted to the mutually exclusive regions in which $\gamma(K)$ is real and pure imaginary.

Let us recall from equation (5.9) that $\gamma(K)$ is the radial wavenumber component of a random disturbance in the ambient medium $r > b$. When γ is pure imaginary such disturbances decay exponentially with radial distance r and do not therefore carry energy away from the jet. The first term on the right of (7.10) for which γ is real, thus accounts for the loss of energy from the coherent jet structure by the radiation of sound waves in free space. The second integral in (7.10) actually consists of a summation over the discrete set of real wavenumbers K which satisfy the dispersion relation

$$F(\omega, K) \equiv \Gamma(\nu - \mu) = 0,$$

and defines the contribution to the decay of the coherent system arising from the generation of trapped, random waves within the jet.

(a) *Conservation of energy*

The above interpretation will now be refined by means of an explicit demonstration of the energy balance between the coherent and random wavefields. Consider Crocco's form of the inviscid momentum equation:

$$\partial \boldsymbol{v}/\partial t + \nabla B = -\boldsymbol{\omega} \wedge \boldsymbol{v} + T\nabla s. \tag{7.11}$$

Here T is the temperature, and s is the specific entropy of the fluid which is constant within the shear layer, $\nabla s \equiv 0$, where also $\boldsymbol{\omega}$ is given by equation (2.17). The energy equation for the random disturbances within the shear layer ($a < r < b$) may be obtained by taking the ensemble average of the scalar product of equation (7.11) with the random momentum fluctuation $\rho_1 \boldsymbol{v}'$. This yields without approximation

$$\tfrac{1}{2}\partial \langle \rho_1 \boldsymbol{v}'^2 \rangle / \partial t + \langle \rho_1 \boldsymbol{v}' \cdot \nabla B' \rangle = -\rho_1 \langle \boldsymbol{v}' \cdot \boldsymbol{\omega} \wedge \bar{\boldsymbol{v}} \rangle. \tag{7.12}$$

Now correct to the second order in the perturbation quantities we have

$$\begin{aligned} \rho_1 \boldsymbol{v}' \cdot \nabla B' &= \operatorname{div}(\rho_1 \boldsymbol{v}' B') - B' \operatorname{div}(\rho_1 \boldsymbol{v}') \\ &= \operatorname{div}(\rho_1 \boldsymbol{v}' B') + (B'/c_1^2)\, \partial p'/\partial t, \end{aligned} \tag{7.13}$$

where use has been made of the equation of continuity and of the adiabatic relation between pressure and density. The perturbation stagnation enthalpy is related to the random pressure fluctuation p' within the shear layer by

$$B' = p'/\rho_1. \tag{7.14}$$

By using (7.13), (7.14) in equation (7.12) and integrating over the volume $\mathscr{V}$ of the shear layer, i.e. the region of the flow in $a < r < b$, it follows that

$$\frac{\partial}{\partial t}\int_{\mathscr{V}} \frac{1}{2}\left\{\rho_1 \langle \boldsymbol{v}'^2 \rangle + \frac{1}{\rho_1 c_1^2}\langle p'^2 \rangle\right\} \mathrm{d}^3\boldsymbol{x} + \oint \langle \rho_1 \boldsymbol{n} \cdot \boldsymbol{v}' B' \rangle \, \mathrm{d}^2\boldsymbol{x} = -\int_{\mathscr{V}} \langle \rho_1 \boldsymbol{v}' \cdot \boldsymbol{\omega} \wedge \bar{\boldsymbol{v}} \rangle \, \mathrm{d}^3\boldsymbol{x}, \tag{7.15}$$

where the second integral on the left is taken over the interfaces $r = a, b$ bounding $\mathscr{V}$, $\boldsymbol{n}$ being the unit outward normal from $\mathscr{V}$.

The first term on the left of (7.15) denotes the rate of change of the mean energy of the random field within the shear layer; in the steady state it must vanish identically. The surface integral is equal to the net flux of random energy from the shear layer (Landau & Lifshitz 1959, §6). The integral involving the triple scalar product accordingly represents the source of the energy of the random field which is located on the surface $r = h$ of the turbulent vorticity layer. It arises from the interaction between the coherent field $\bar{\boldsymbol{v}}$, the turbulent fluctuations $\boldsymbol{\omega}$ and the random field $\boldsymbol{v}'$,

and is equal to the power flux $\mathscr{P}$, say, from the coherent jet structure into the random scattered disturbances. Thus we may write

$$\mathscr{P} = -\rho_1 \int_{\mathscr{V}} \langle \boldsymbol{v}' \cdot \boldsymbol{\omega} \wedge \bar{\boldsymbol{v}} \rangle \, \mathrm{d}^3\boldsymbol{x}$$
$$\equiv \rho_1 \int_{\mathscr{V}} \bar{\boldsymbol{v}} \cdot \langle \boldsymbol{\omega} \wedge \boldsymbol{v}' \rangle \, \mathrm{d}^3\boldsymbol{x}. \tag{7.16}$$

This integral may be simplified by making use of equation (5.21) giving the value of $\boldsymbol{v}'$ at the vorticity layer. We shall consider the case as the shear layer width $\delta = b - a \to 0$. The details of the evaluation of the mean value $\langle \boldsymbol{\omega} \wedge \boldsymbol{v}' \rangle$ are entirely analogous to those outlined in §5 during the determination of the mean interaction functions $\chi_1(k)$, $\chi_2(k)$. In the present approximation, in which the right-hand side of (7.16) is to be evaluated correct to $O(\epsilon^2)$, the coherent velocity $\bar{\boldsymbol{v}}$ may be taken to be that given by equation (6.7) and, on taking account of the expression (6.17) leads to

$$\bar{\boldsymbol{v}} = \frac{-P}{2\pi \mathrm{i} \rho_1} \int_{-\infty}^{\infty} \frac{\mathrm{e}^{\mathrm{i}k(x+Vt)}}{\omega J_0(\beta_1 ka - \mathrm{i}\Delta_0(k))} \left(J_0(\beta_1 ka), \frac{\mathrm{i}\beta_1 V^2}{U^2} J_1(\beta_1 ka) \right) \mathrm{d}k. \tag{7.17}$$

Observe that $\bar{\boldsymbol{v}}$ occurs twice in the integrand of (7.16), once as indicated explicitly, and also in the representation (5.21) of $\boldsymbol{v}'$ where $B^{(2)}$, C are defined in terms of $\bar{\boldsymbol{v}}$ by means of the relations (5.19), (5.12).

The steps in the simplification of the power flux integral (7.16) are tedious but straightforward, and present no difficulties not already encountered in §§5, 6. Performing the reduction we find that as $\delta \to 0$, $\mathscr{P}$ may be expressed in terms of the double wavenumber integral

$$\mathscr{P} = -\frac{\mathrm{i}aP^2}{2\rho_1} \iint_{-\infty}^{\infty} \frac{\Phi(k-K)}{\omega^3 \Gamma(\nu-\mu) |J_0(\beta_1 ka + \mathrm{i}\Delta_0(k))|^2} \Big\{ \Gamma^2 \nu\mu J_0(\beta_1 ka)^2$$
$$+ \frac{\beta_1 K \Gamma V^2}{U^2} (\nu+\mu) \, J_0(\beta_1 ka) \, J_1(\beta_1 ka) + \frac{\beta_1^2 K^2 V^4}{U^4} J_1(\beta_1 ka)^2 \Big\} \, \mathrm{d}K \, \mathrm{d}k + \text{c.c.} \tag{7.18}$$

where $\omega = -Vk$.

But $\Delta_0(k) \sim O(\epsilon^2)$ so that the integrand in this result is $O(\epsilon^2)$ except in the vicinity of the zeros of $J_0(\beta_1 ka)$ where it $\sim O(1/\epsilon^2)$. Hence, since ϵ is small the principal contribution to $\mathscr{P}$ is provided by those values of k where $J_0(\beta_1 ka)$ is small, and in this case only the final term in the curly brackets of the integrand is significant. Thus in the leading approximation

$$\mathscr{P} = -\frac{\mathrm{i}aP^2\beta_1^2 V^4}{2\rho_1 U^4} \iint_{-\infty}^{\infty} \frac{K^2 \Phi(k-K) \, J_1(\beta_1 ka)^2}{\omega^3 |J_0(\beta_1 ka + \mathrm{i}\Delta_0(k))|^2} \left\{ \frac{1}{\Gamma(\nu-\mu)} - \text{c.c.} \right\} \mathrm{d}K \, \mathrm{d}k. \tag{7.19}$$

Comparing this with the integral (7.2) for the dissipation function $\Delta_0(k)$ we also have

$$\mathscr{P} = \frac{aP^2\beta_1 V}{\rho_1 U^2} \int_{-\infty}^{\infty} \frac{\Delta_0(k) \, J_1(\beta_1 ka)^2 \, \mathrm{d}k}{k^2 |J_0(\beta_1 ka + \mathrm{i}\Delta_0(k))|^2}, \tag{7.20}$$

where use has been made of the coherent field relation $\omega = -Vk$.

Consider first the situation in which the turbulence Mach number $\epsilon \to 0$. This also implies that $\Delta_0(k) \to 0$. The physical constraint of irreversibility (second law of thermodynamics) requires the dissipation function $\Delta_0(k)$ to be non-negative. Hence as $\epsilon \to +0$ we may use the limiting identity of equation (2.29) to express (7.20) in the form

$$\mathscr{P} = \frac{2\pi a^2 \beta_1^2 P^2 V}{\rho_1 U^2} \sum_{n=1}^{\infty} \frac{1}{\lambda_n^2} \equiv \frac{\pi a^2 \beta_1^2 P^2 V}{2\rho_1 U^2}, \tag{7.21}$$

λ_n ($n \geqslant 1$) being the nth positive zero of $J_0(z)$. This expression for the power flux into the random field is identical to that given in (2.30) for the flux of energy into the coherent jet structure from the incident pressure wave (2.21). In other words, as the turbulence Mach number $\epsilon \to 0$ the total scattered energy is precisely equal to the flux of energy into the coherent wave system which decays downstream of the nozzle.

For small but finite values of ϵ the δ function identity used in reducing (7.20) to (7.21) cannot strictly be applied. This is because the spectral peaks of the coherent field have been broadened by radiation damping. The peaks are located at $\beta_1 k_n a = \lambda_n$ and the corresponding width of the spectral line is proportional to $\Delta_0(k_n)$. The input of energy to the coherent field from the incident wave (2.21) must now be determined from the expressions which define the mean jet structure in the presence of scattering, i.e. by making use of equation (6.18) of the previous section. It is then a simple matter to deduce from the energy flux integral of (2.23) that the integral expression (7.20) also defines the flux of energy into the coherent waves from the incident wave (2.21).

However, it is clear that even when the root mean square turbulence Mach number ϵ is finite the principal contributions to the integral (7.20) come from the regions $k \approx k_n$, and therefore that its value will not deviate substantially from (7.21). In other words the precise rate of decay of the cell structure does not significantly affect the level of the total scattered sound power.

8. The radiation of sound into free space

We now apply the results of the previous sections to determine the sound radiated into free space. In this respect we are principally interested in the properties of the acoustic field which is the direct scattering product of the turbulent shear layer and the coherent shock-cell structure of the jet.

The internally scattered random wave modes subsequently experience multiple scattering and thereby provide an additional source of free space acoustic radiation. The sound generated in this way is significant, and must actually be comparable with that scattered directly from the coherent wave system. However, the effect of multiple interactions is to spread the random internal wave energy over a wide range of frequencies, and consequently the spectrum of the accompanying free space sound field will be 'broad-band'. On the contrary the spectrum of shock associated noise exhibits a sequence of peaks which in terms of the present theory must be associated with the coherent scattering of sound by the array of shock cells. It is this aspect of the radiated sound that is investigated in this section.

This component of the free space radiation may in principle be determined from the inverse Fourier transform of equation (5.9), namely,

$$\varphi' = \iint_{-\infty}^{\infty} T(\omega, K)\, H_0^{(1)}(\gamma r)\, \mathrm{e}^{\mathrm{i}(Kx-\omega t)}\, \mathrm{d}K\, \mathrm{d}\omega, \tag{8.1}$$

where the coefficient $T(\omega, K)$ is determined by the system of equations (5.14), (5.15). In practice only the mean square properties of the radiation are required, and we may avoid the analytical complications associated with the complete representation (8.1) of the sound field by making use of the power flux integral (7.20) of the previous section.

That integral gives the contribution to the total scattered sound from each wavenumber component k of the coherent wavefield (6.18). The spectral distribution of the random fluctuations generated by each of these components is furnished by the dissipation function $\Delta_0(k)$ occurring in the numerator of the integrand of (7.20). Indeed, $\Delta_0(k)$ has been shown to possess the

integral representation (7.10). The first integral on the right of (7.10) is over those values of the wavenumber K of the scattered field which propagate as sound in free space; the second integral corresponds to the internally scattered waves.

Introduce the definition

$$Z_0(k, K) = \frac{K^2(\rho_1/\rho_0)}{|\Gamma|^2|\nu-\mu|^2|H_0^{(1)}(\gamma a)|^2}\left(\frac{\omega}{\omega+VK}\right)^2 \geqslant 0. \tag{8.2}$$

Then if $\mathscr{P}_A$ denotes the power flux into the free space acoustic modes, it follows from (7.20), (7.10) that

$$\mathscr{P}_A = \frac{2P^2\beta_1^2 V^4}{\pi\rho_1 U^4}\int^{\mathrm{Re}(\gamma)} \frac{\mathrm{sgn}\,(\gamma)\,\Phi(k-K)\,J_1(\beta_1 ka)^2}{\omega^3|J_0(\beta_1 ka+\mathrm{i}\Delta_0(k)|^2} Z_0(k, K)\,\mathrm{d}K\,\mathrm{d}k. \tag{8.3}$$

Next observe that for each of the scattered sound waves in free space $(K, \gamma(K))$ represents the (x, r) component of the acoustic wavenumber vector, where since γ is real, we have from (5.10)

$$\gamma(K) = \mathrm{sgn}\,(\omega+VK)\,|(\omega+VK)^2/c_0^2 - K^2|^{\frac{1}{2}} \tag{8.4}$$

In this expression $\omega \equiv -Vk$ is the radian frequency of the scattered wave in the x-reference frame which is at rest relative to the turbulent shear layer. In a system of coordinates which is stationary with respect to free space, the shear layer translates in the positive x-direction at velocity V. Consequently the radian frequency Ω, say, of the sound wave relative to the ambient medium is given by the Doppler formula

$$\Omega = \omega + VK, \tag{8.5}$$

from which we have

$$k = -(1/V)(\Omega - VK). \tag{8.6}$$

Making this substitution in (8.3) we obtain

$$\mathscr{P}_A = -\frac{2P^2\beta_1^2}{\pi\rho_1 U^4}\int^{\mathrm{Re}(\gamma)} \frac{\mathrm{sgn}\,(\gamma)\,\Phi(\bar{k}-K)\,J_1(\beta_1\bar{k}a)^2\,Z_0(\bar{k}, K)\,\mathrm{d}K\,\mathrm{d}\Omega}{\bar{k}^3|J_0(\beta_1\bar{k}a+\mathrm{i}\Delta_0(\bar{k}))|^2}, \tag{8.7}$$

where $\bar{k}$ is defined by the right-hand side of (8.6).

Equation (8.7) represents the scattered power as an integral over the x component of the acoustic wavenumber vector and the frequency Ω relative to an observer fixed in free space. Accordingly, if θ denotes the direction of propagation in free space, i.e. θ is the polar angle of the normal to the wavefront measured from the positive x-axis, we have from (8.4)

$$\left.\begin{aligned} K &= (\Omega/c_0)\cos\theta, \\ \gamma &= (\Omega/c_0)\sin\theta, \end{aligned}\right\} \tag{8.8}$$

where $0 \leqslant \theta \leqslant \pi$, which includes all possible values of K for which $\gamma(K)$ is real. Using this in the integral (8.7) gives

$$\mathscr{P}_A = \frac{4P^2\beta_1^2 V^3}{\pi\rho_1 U^4 c_0}\int_0^\infty \mathrm{d}\Omega \int_0^\pi \frac{\Phi(\Omega/V)\,J_1(\beta_1\bar{k}a)^2}{\Omega^2(1-M_0\cos\theta)^3|\,J_0(\beta_1\bar{k}a+\mathrm{i}\Delta_0(\bar{k}))|^2} Z_0\left(\bar{k}, \frac{\Omega}{c_0}\cos\theta\right)\sin\theta\,\mathrm{d}\theta, \tag{8.9}$$

where now $\bar{k} = -(\Omega/V)(1-M_0\cos\theta)$, $M_0 = V/c_0$ is the shear layer Mach number relative to the sound speed c_0 in free space, and it has been noted that the integrand is an even function of Ω.

The acoustic power flux $\mathscr{P}_A$ is given in (8.9) as an integral with respect to the frequency Ω and all possible radiation directions θ. The integrand is positive definite provided that the shear layer is subsonic ($M_0 < 1$). In the supersonic case the integrand becomes negative for

$$\theta < \arccos\{1/M_0\},$$

PHILOSOPHICAL TRANSACTIONS OF THE ROYAL SOCIETY A MATHEMATICAL, PHYSICAL & ENGINEERING SCIENCES

which is the Mach angle for a source translating at velocity V in the positive x-direction. This angle lies within the classical free space zone of silence $0 < \theta < \theta_s$, for acoustic sources located within the jet, where $\theta_s = \arccos\{c_0/(c_1+U)\}$ (see, for example, Morse & Ingard 1968, §11.1).

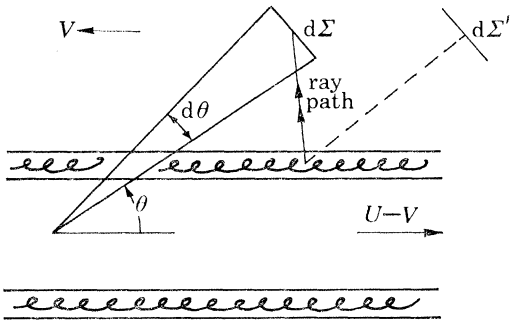

FIGURE 3. Section through the jet and the elementary control surface $d\Sigma(\theta)$ which is fixed relative to the ambient medium. $d\Sigma'$ denotes the position of the surface element at the time of emission of sound by a source located at rest relative to shear layer The 'ray path' is the path of propagation relative to a reference frame fixed with respect to the shear layer.

In order to see the physical significance of the negative power flux consider a packet of scattered waves which propagates relative to the ambient medium within an interval $d\theta$ of the direction θ (figure 3). Let these waves pass through an elementary control surface $d\Sigma(\theta)$ which is fixed relative to the ambient medium and occupies the sector $(\theta, d\theta)$ of the surface of a large sphere of radius R centred on the axis of the jet, i.e. such that

$$d\Sigma = 2\pi R^2 \sin\theta\, d\theta.$$

Then the radius R through $d\Sigma$ lies in the direction of the wavenormal of the incident sound waves. These waves actually arrive at $d\Sigma$ after propagating along the ray path illustrated in figure 3 which takes account of the mean flow of the ambient medium at velocity V in the negative x-direction. It follows that for an observer at rest relative to the ambient flow and who is instantaneously located at $d\Sigma$ at the time of arrival of the sound waves, (R, θ) represent his polar position relative to the source of sound *at the time of emission of the radiation*. In otherwords, since the nozzle is fixed in free space, (R, θ) specify the fixed observer location relative to the nozzle.

The ensemble average of the flux of energy through $d\Sigma$ may be deduced directly from (8.9) by noting that it corresponds to the interval $(\theta, d\theta)$ of the θ-integration:

$$d\mathscr{P}_A(\theta) = \frac{2P^2\beta_1^2 V^3 d\Sigma}{\pi^2 R^2 \rho_1 U^4 c_0}\int_0^\infty \frac{\Phi(\Omega/V)\, J_1(\beta_1 \bar{k}a)^2\, Z_0(\bar{k}, \Omega\cos\theta/c_0)\, d\Omega}{\Omega^2(1-M_0\cos\theta)^3 |J_0(\beta_1\bar{k}a + i\Delta_0(\bar{k}))|^2}. \tag{8.10}$$

We can also express $d\mathscr{P}_A(\theta)$ in terms of the mean square pressure perturbation $\langle p^2\rangle \equiv \overline{p^2}$. The flux of energy through $d\Sigma$ due to the radiation in $(\theta, d\theta)$ is made up of two components:

$d\mathscr{P}_A$ = rate at which work is done on $d\Sigma$ by the fluctuating pressure p + the rate at which acoustic energy is convected through $d\Sigma$ by the mean flow at velocity V in the negative x-direction. (8.11)

The first term on the right hand side is equal to

$$(\overline{p^2}/\rho_0 c_0)\, d\Sigma.$$

Also the acoustic energy density is $\overline{p^2}/\rho_0 c_0^2$, and the rate at which acoustic energy is convected through $\mathrm{d}\Sigma$ is therefore equal to

$$(\overline{p^2}/\rho_0 c_0^2)\,(-V\cos\theta)\,\mathrm{d}\Sigma.$$

Thus (8.11) becomes

$$\mathrm{d}\mathscr{P}_{\mathrm{A}}(\theta) = \frac{\overline{p^2}}{\rho_0 c_0}(1 - M_0\cos\theta)\,\mathrm{d}\Sigma. \tag{8.12}$$

It is clear that this can be negative when $M_0 > 1$ and for $\theta < \arccos\{1/M_0\}$, and this case arises when the convection term of (8.11) exceeds the rate of working by the pressure fluctuations.

Next we may equate the results (8.10), (8.12) to obtain the following spectral representation of the mean square pressure fluctuation

$$\overline{p^2} = \frac{2P^2\beta_1^2\rho_0 V^3}{\pi^2 R^2 \rho_1 U^4}\int_0^\infty \frac{\Phi(\Omega/V)\,J_1(\beta_1\bar{k}a)^2\,Z_0(\bar{k}, \Omega\cos\theta/c_0)\,\mathrm{d}\Omega}{\Omega^2(1 - M_0\cos\theta)^4\,|J_0(\beta_1\bar{k}a + \mathrm{i}\Delta_0(\bar{k}))|^2}. \tag{8.13}$$

Note that the integrand is positive definite. Equation (8.13) constitutes the frequency distribution of the sound pressure level for an observer located at rest in the distant field at the polar position (R, θ) relative to the nozzle of the jet. The spectrum is characterized by a sequence of sharp peaks $\sim O(1/\epsilon^2)$ which occur at those values of $\bar{k}$ at which $J_0(\beta_1\bar{k}a) = 0$, i.e. for

$$\Omega = \frac{\lambda_n V}{\beta_1 a|1 - M_0\cos\theta|}.$$

Note that the principal contribution to the acoustic spectrum is associated with the low wavenumber components λ_n of the Fourier series representation (2.14) of the shock-cell system. This may be contrasted with Lighthill's (1953) result that the spectrum of the direct scattered sound produced by the interaction of turbulence with a weak shock wave is dominated by the high wavenumber components of the incident wave. The difference arises because in the shock noise problem the largest component of the radiation field is provided by scattering events which are correlated over large distances, namely of the order of the characteristic wavelength of the shock cells.

Let us now examine the physical significance of the limiting approximation $\delta = b - a \to 0$ of vanishing shear layer width which has been applied here and in §§6, 7. First note from (8.2) that since

$$K = (\Omega/c_0)\cos\theta \quad (0 \leqslant \theta \leqslant \pi),$$

the function $Z_0(\bar{k}, \Omega/c_0\cos\theta)$ which appears in the spectral representation (8.13) vanishes in the radiation direction $\theta = 90°$. The reason for this may be understood by noting that the coherent field velocity perturbation $\bar{\boldsymbol{v}} = (\bar{u}, \bar{v})$ at the turbulent vorticity layer is given in the limit as $\delta \to 0$ by equation (6.7). Referring to the integral form (6.18) of the coherent field we see that it is determined principally by those wavenumbers k located near the zeros of $J_0(\beta_1 ka)$, and this in turn implies that at $r = a$ the axial component $\bar{u}$ of the coherent velocity is small; in fact $\bar{u} \sim O(\epsilon^2)\,\bar{v}$ Hence the only significant contribution to the source term on the right hand side of the local Born approximation (5.5) for the random scattered field is

$$\mathrm{div}\,(\boldsymbol{\omega} \wedge \bar{\boldsymbol{v}}) = -\delta(r - a)\,\partial[\xi(x)\,\bar{v}(x, t)]/\partial x. \tag{8.15}$$

Accordingly the source consists of a random distribution of acoustic 'dipoles' orientated parallel to the jet axis and for which $\theta = 90°$ is a null radiation direction.

The radiation at right angles to the jet axis is associated with radially orientated dipoles of the form

$$\operatorname{div}(\boldsymbol{\omega}\wedge\bar{\boldsymbol{v}}) = (h/r)\,\partial\{\xi(x)\,\bar{u}(x,t)\,\delta(r-h)\}/\partial r. \tag{8.16}$$

These can arise in the theoretical modelling of shock associated noise considered in this paper only when account is taken of the finite width $\delta = b-a$ of the turbulent shear layer. The corresponding modifications to the results obtained above will now be discussed.

9. The effect of finite shear layer width

We shall assume that $k\delta$ is small and obtain only the first order corrections to previous results in which δ was taken to be zero. The analysis is simplified by taking the limit $h\to a$, in which the random turbulent vorticity layer ultimately coincides with the inner interface $r = a$. Observe that it would be inappropriate to let $h\to b$ since this would imply that $\bar{u}$ is negligible at the turbulent shear layer and would again give no radiation at right angles to the jet axis.

Consider first the coherent field interaction equation (4.23). For small values of $k\delta$ the first two terms on the left-hand side become in the leading approximation

$$\begin{aligned}\mathscr{A}_- H_0^{(1)}(\beta_2 ka) + \mathscr{B}_- H_0^{(2)}(\beta_2 ka) - \beta_2 k\delta\{\mathscr{A}_- H_1^{(1)}(\beta_2 ka) + \mathscr{B}_- H_1^{(2)}(\beta_2 ka)\}\\ = (U/V)\,\mathscr{D}\{J_0(\beta_1 ka) - \beta_1(V/U)^2 k\delta J_1(\beta_1 ka)\},\end{aligned} \tag{9.1}$$

where use has been made of equations (4.16), (4.18). The expression on the right of (9.1) is approximately equal to

$$(U/V)\,\mathscr{D}J_0(\beta_1 k[a+\delta(V/U)^2]),$$

and it follows that when scattering by the turbulent shear layer is ignored (i.e. when $\chi_1(k)$, $\chi_2(k)$ are set equal to zero in (4.23)), the Fourier coefficient $\mathscr{D}(k)$ of the coherent field within the jet flow ($r < a$) is given by

$$\left.\begin{aligned}\mathscr{D}(k) &= \frac{VS}{\rho_1 UJ_0(\beta_1 k\bar{a})},\\ \bar{a} &= a+\delta(V/U)^2.\end{aligned}\right\} \tag{9.2}$$

This provides the first order correction to the analogous result (6.11) which obtains when $\delta = 0$.

When the remaining contributions to equation (4.23) are approximated for small, but finite $k\delta$, the principal non-trivial modifications of the earlier results are found to be as follows.

(i) The dissipation function $\Delta_0(k)$ of equation (6.13) becomes

$$\Delta_1(k) = \operatorname{Im}\left\{-\frac{\beta_1 V^2 k}{U^2\omega^2}\int_{-\infty}^{\infty}\Phi(k-K)\left[\frac{K^2}{\Gamma(\nu-\mu)}+\frac{(k\delta)^2}{(1/\Gamma\mu-1/\Gamma\nu)}\right]\mathrm{d}K\right\}. \tag{9.3}$$

(ii) In equations (6.17), (6.18) for the coherent structure within the jet flow, and in the integrand of the power flux integral (7.20), a is replaced by $\bar{a}$, and $\Delta_0(k)$ is replaced by $\Delta_1(k)$.

(iii) Equations (8.3), (8.10), (8.13) which define the free space acoustic power $\mathscr{P}_A$ and the spectral composition of the radiation field, are modified by replacing a by $\bar{a}$, $\Delta_0(k)$ by $\Delta_1(k)$, and the function $Z_0(k, K)$ defined in (8.2) is replaced by $Z_1(k, K)$, where

$$Z_1(k,K) = Z_0(k,K) + \frac{(k\delta)^2(\rho_0/\rho_1)}{|\gamma|^2|H_1^{(1)}(\gamma a)|^2|1/\Gamma\mu-1/\Gamma\nu|^2}\left(\frac{\omega+VK}{\omega}\right)^2. \tag{9.4}$$

In particular note that for $K = (\Omega/c_0)\cos\theta$, the second term on the right of (9.4) is non-zero at $\theta = 90°$. Hence the modified form of the spectral representation (8.13) of the acoustic field possesses a finite contribution in this radiation direction.

10. Practical implications of the analysis: shock associated noise of a supersonic transport

In this section the results of the theoretical investigation described above are considered in relation to the jet noise of a supersonic transport such as *Concorde*. Naturally it is not possible to make a precise identification of the parameters of the model problem with those describing the gross features of a real jet, but the error involved here is very much less than that already introduced into the analysis by the idealized representation of the turbulent shear layer. We shall examine in particular the following aspects of the free space radiation:

(i) the spectrum of the direct scattered sound;

(ii) the directivity or field shape of the direct scattered sound and its dependence on the forward flight velocity of the aircraft;

(iii) the total acoustic power associated with the presence of shock cells.

Recall that 'direct scattered sound' refers to that component of the radiation field generated by the direct interaction of the turbulence and the shock cells (see §8), and which is usually referred to as *the* shock associated noise (Harper, Bourne & Fisher 1973).

(*a*) *The turbulence spectrum and the dissipation function* $\Delta_1(k)$

We must first specify a functional form for the turbulence spectrum $\Phi(k)$ defined by equation (2.20). The model shear layer consists of a mean flow at velocity V in which is convected a frozen field of axi-symmetric vorticity ω given by (2.17). The mean vorticity of the shear layer is equal to U/δ, where δ is the width of the layer. The random function $\xi(x)$ describes the local fluctuation about this mean value and the total circulation associated with ω must vanish:

$$\int_{-\infty}^{\infty} \xi(x)\,\mathrm{d}x = 0. \tag{10.1}$$

From (2.19), (2.20) this condition implies that $\Phi(k) \to 0$ as $k \to 0$ and we shall introduce the following simple analytical representation of the spectrum which is consistent with this constraint:

$$\Phi(k) = \frac{\langle \xi^2 \rangle l}{\pi^{\frac{3}{2}}} \left(\frac{kl}{2\pi}\right)^2 \exp\left\{-\left(\frac{kl}{2\pi}\right)^2\right\}. \tag{10.2}$$

This attains its maximum value at $k = 2\pi/l$, corresponding to dominant vortical disturbances of wavelength l.

Next it is necessary to determine the explicit form of the dissipation function $\Delta_1(k)$ which appears in the spectral representation of the direct scattered sound in the manner discussed in §§8, 9. This is given by equation (9.3). That result may be expressed in terms of separate contributions from the direct scattered sound and the internally scattered wave modes as in the case of the analogous decomposition (7.10) of $\Delta_0(k)$.

Consider for definiteness the representation (7.10). For a fixed value of the wave number k both integrals may be calculated numerically. The first, giving the contribution to $\Delta_0(k)$ from the direct scattered sound, poses no serious problem in this respect. The second integral may be evaluated formally because of the presence of the δ function in the integrand, the contributions arising from the real zeros of the dispersion function $F(\omega, K)$. Recalling that $\omega = -Vk$, it follows that these zeros occur in the range of K satisfying (for $k > 0$).

$$K > M_0 k/(M_0+1) \quad \text{or} \quad K < M_0 k/(M_0-1) \tag{10.3}$$

for which $\gamma(K)$ is pure imaginary. The numerical problem in this case thus reduces to the determination of these zeros. Procedures for doing this have been considered in a similar context by Morgan (1975) and Munt (1977) and involve a considerable amount of numerical computation. In view of the idealized nature of the model problem a thorough numerical investigation can hardly be justified in the present case since the gain in the precision of the final result is unlikely to compensate for the deficiencies in the theoretical modelling of the turbulent shear layer.

In order to avoid these difficulties note first of all that the point $K = k$ is always included in the range (10.3) for which $\gamma(K)$ is pure imaginary. This indicates that, if the spectrum function $\Phi(k-K)$ decays rapidly as $|K-k|$ increases, the principal contributions to the dissipation function $\Lambda_0(k)$ would be furnished by the second of the integrals in (7.10), i.e. the generation of internally scattered waves would be primarily responsible for the decay of the shock cells. For this to be the case it is necessary for $kl/2\pi$ to be large, where l is the dominant wavelength of the turbulent field introduced above. But the integrand of (8.13) shows that the precise value of $\Lambda_0(k)$ is significant only when $\beta_1 ka$ lies in the neighbourhood of a zero λ_n say, of $J_0(z)$. The relevant condition is therefore

$$(\lambda_n/2\pi\beta_1)\,(l/a) \gtrsim 1. \tag{10.4}$$

The turbulent scale l is of the same order as the nozzle diameter $2a$, and in the applications to be considered below β_1 will not exceed unity. It follows that (10.4) should be valid for those λ_n for which $n > 1$.

Thus the dissipation function $\Lambda_0(k)$ is essentially determined by the second integral of (7.10), which in turn reduces to a summation over terms corresponding to the real zeros of $F(\omega, K)$ where $\omega \equiv -Vk$. The rapid decay of $\Phi(k-K)$ means that only those zeros close to $K = k$ need be taken into account. Let $N(k)$ denote the number of zeros involved here, for which $\Phi(k-K) \sim \langle \xi^2 \rangle l$. A consideration of the dimensions of the quantities appearing in the second integrand of (7.10) then leads to the following parametric dependence of the dissipation function:

$$\Lambda_0(k) \propto \epsilon^2 lkN(k), \tag{10.5}$$

ϵ being the turbulence Mach number. A similar argument applied in the case of small, but finite shear layer width δ implies an analogous parametric form for the corresponding dissipation function $\Lambda_1(k)$.

The number of zeros $N(k)$ increases approximately linearly with wavenumber k, corresponding to the increasing frequency of oscillation of the Bessel functions $J_0(\Gamma_J a)$, $J_1(\Gamma_J a)$ which occur in the definition (7.1) of the dispersion function $F(\omega, K) \equiv \Gamma(\nu-\mu)$ (cf. Morgan 1975). Noting also that the growth of the turbulent eddies will be dependent on the length scale of the mean flow through which they translate, so that l may be expected to be proportional to the scale $\beta_1 a$ of the shock cells, we therefore obtain the following approximate representation of the dissipation function

$$\Lambda_1(k) = \alpha(\beta_1 ka)^2, \tag{10.6}$$

where α is constant.

An estimate for the value of the coefficient α may be derived by making use of the description (2.14) of the boundary of an imperfectly expanded jet. Pack (1950) has shown by numerical computation that the first minimum in the boundary displacement (i.e. the point marked A in figure 1*b*) occurs at a distance of approximately

$$L = 2.4\beta_1 a \tag{10.7}$$

from the nozzle. This will be assumed to characterize the length of a typical shock cell. According to Trevett (1968) the number of well formed cells is typically of order 8. By using this figure α may be estimated by assuming that the exponential decay of the principal Fourier coefficient ($n = 1$) of (2.14) has reduced in value by a factor of 0.5 over half the total length of the array of cells, i.e. for $x_1 = 4L$. This implies that $d_1 = 0.072$. Hence noting that $d_1 = \Delta_1(\lambda_1/\beta_1 a)$ where $\lambda_1 = 2.4048$ is the first zero of $J_0(z)$, it follows from (10.6) that

$$\alpha = 0.0125 \tag{10.8}$$

Let us note here, with reference to the results of (ii) in §10*b* concerning the intensity of the direct scattered sound, that increasing/decreasing the effective length of the system of shock-cells by 50% from the above figure only results in an increase/decrease of about 2 dB and 3 dB respectively in the direct scattered sound pressure level.

(*b*) *Underexpanded jet flow characteristics of a supersonic transport*

The jet of a supersonic transport such as *Concorde* consists of an underexpanded supercritical flow exhausting from an approximately conical nozzle. The throat of the flow therefore occurs at the nozzle exit and the flow there is sonic. As discussed in detail by Pack (1950), the jet velocity which determines the mean Mach number M_J of the free jet-flow is correctly approximated by the fully-expanded jet velocity which in the model analysis occurs at the boundary of the jet where the pressure is equal to the atmospheric pressure p_A, say.

Table 1 lists the principal characteristics of a supersonic jet such as that of the Rolls Royce–SNECMA *Olympus* 593 engine which powers the *Concorde*. The entries are taken from Jacques (1977), and correspond to conditions appropriate to three modes of engine operation. At take-off the engine can be operated with or without 're-heat'. In the re-heat mode additional fuel is injected upstream of the nozzle exit to provide increased thrust. The cut-back condition refers to the procedure whereby the thrust is reduced after take-off to comply with noise abatement regulations.

TABLE 1

mode	pressure ratio, p_J/p_A	γ	$\frac{T_J}{K}$	$\frac{T_d}{K}$	M_J	$\frac{C_p}{(J\ kg^{-1}\ K^{-1})}$	$\frac{S}{m^2}$	$\frac{Q/S}{(kg\ s^{-1}\ m^{-2})}$
cut-back	2.4	1.350	815	650	1.21	1074	0.583	340.0
take-off	3	1.319	1100	843	1.38	1125	0.560	362.4
re-heat	3	1.295	1450	1112	1.39	1158	0.638	319.2

The quantities appearing in table 1 are defined as follows:

p_J = total jet pressure,
γ = ratio of specific heats,
T_J = total jet temperature/K
T_d = temperature of fully expanded jet/K,
C_p = specific heat at constant pressure/(J kg^{-1} K^{-1}),
S = nozzle exit area/m^2
Q = mass flow/(kg s^{-1}).

In the following discussion we shall take the ambient medium to be a standard atmosphere $\gamma_{air} = 1.40$, $T_{air} = 15\,^{\circ}C$, $p_A = 101\,300$ N/m^2.

(i) *The spectrum of the direct scattered sound*

Let us now illustrate the spectral distribution of the direct scattered sound predicted by the model analysis. This is given by the integrand of (8.13) with Z_0 replaced by the finite shear layer expression Z_1 defined in (9.4). The acoustic frequency $f \equiv \Omega/2\pi$ will be normalized with respect to that of the principal peak of the spectrum of the sound scattered in the $\theta = 90°$ direction. From (8.14) that peak occurs at $f \equiv f_p$, say, where

$$f_p = \lambda_1 V/2\pi\beta_1 a = V/1.31D\beta_1, \tag{10.9}$$

$D = 2a$ being the nozzle exit diameter. In the θ direction the peak is displaced to

$$f_p(\theta) = \frac{f_p}{|1 - M_0 \cos\theta|} \equiv \frac{V}{1.31D\beta_1|1 - M_0\cos\theta|}. \tag{10.10}$$

This formula exhibits the same functional dependence on D, β_1 and the eddy convection velocity V as that predicted by Harper Bourne & Fisher (1973) from their empirical modelling of shock associated noise. In their formula, however, the numerical coefficient 1.31 is replaced by 1.1. According to recently published experimental data of Tanna (1977), both formulae underestimate the actual peak frequency (Tanna suggests 0.87 for the value of the numerical coefficient) although the data tend to confirm the functional dependence of $f_p(\theta)$ on V, β_1 and θ.

The successive peaks of the predicted spectrum are not equally spaced as they would be for a harmonic sequence. This is because the nth peak frequency is proportional to the wavenumber $\lambda_n/\beta_1 a$ of the nth component of the Fourier series expansion (2.14) of the shock cell structure, where, as before, for a circular jet the λ_n denote the zeros of $J_0(z)$. In the case of a hot jet only the first peak can normally be distinguished against the background of the broad-band jet mixing noise. For a cold jet the second peak is discernible in some radiation directions (Harper Bourne & Fisher 1973) and occurs at $f = 2.3 f_p(\theta)$.

The spectrum of the direct scattered sound is given by the integrand of (8.13) (with Z_1 replacing Z_0). Experiments usually provide a '$\frac{1}{3}$-octave' representation of the acoustic spectrum so that in order to obtain a comparison with the theory the integrand of (8.13) should be multiplied by the frequency, f. The product may be represented in the following non-dimensional form

$$\Psi\left(\frac{f}{f_p}, \theta\right) = \left(\frac{\rho_0}{\rho_1}\right)\left(\frac{f}{f_p}\right) Z_1\left(\bar{k}, \frac{\Omega\cos\theta}{c_0}\right) \exp\left\{-\left(\frac{f}{f_p}\right)^2\left(\frac{\lambda_1 l}{2\pi\beta_1 a}\right)^2\right\}$$
$$\times \frac{J_1(\beta_1\bar{k}a)^2}{(1 - M_0\cos\theta)^4|J_0(\beta_1\bar{k}a + \mathrm{i}\alpha(\beta_1\bar{k}a)^2)|^2}. \tag{10.11}$$

in which

$$\left.\begin{aligned} \Omega &= (f/f_p)\,(\lambda_1 V/\beta_1 a), \\ \bar{k} &= -\frac{\Omega}{V}(1 - M_0\cos\theta) \equiv -\frac{(f/f_p)\,\lambda_1(1 - M_0\cos\theta)}{\beta_1 a} \end{aligned}\right\} \tag{10.12}$$

and it is assumed that the eddy convection velocity $V = 0.6U$. It is readily verified from the definitions (8.2), (9.4) that when the frequency f is normalized in the above manner the explicit dependence of $Z_1(\bar{k}, \Omega\cos\theta/c_0)$ on the radius a of the nozzle occurs only through the ratio δ/a involving the shear-layer width.

Consider first a *cold* jet in which the static temperature of the fully expanded flow is equal to that of the atmosphere. Harper Bourne & Fisher (1973) have investigated this case experimentally for $\beta_1 \equiv \sqrt{(M_J^2 - 1)} = 1$, $(M_J = \sqrt{2})$. Figure 4 depicts measured spectra at a distance of

118 nozzle exit diameters from the nozzle at $\theta = 45°$, 90° and 135°. To compare these with corresponding spectra predicted by (10.11) we consider the case in which $\delta/a = 0.02$, and $l/a = 1.7$, where l is the eddy length scale. This furnishes approximate agreement between theory and experiment at $\theta = 135°$, after which (10.11) determines the absolute spectral levels for all radiation directions. The theoretical spectra are also plotted in figure 4, and exhibit the characteristic peaks discussed above, the location of the principal peak $f_p(\theta)$ varying in accordance with (10.10).

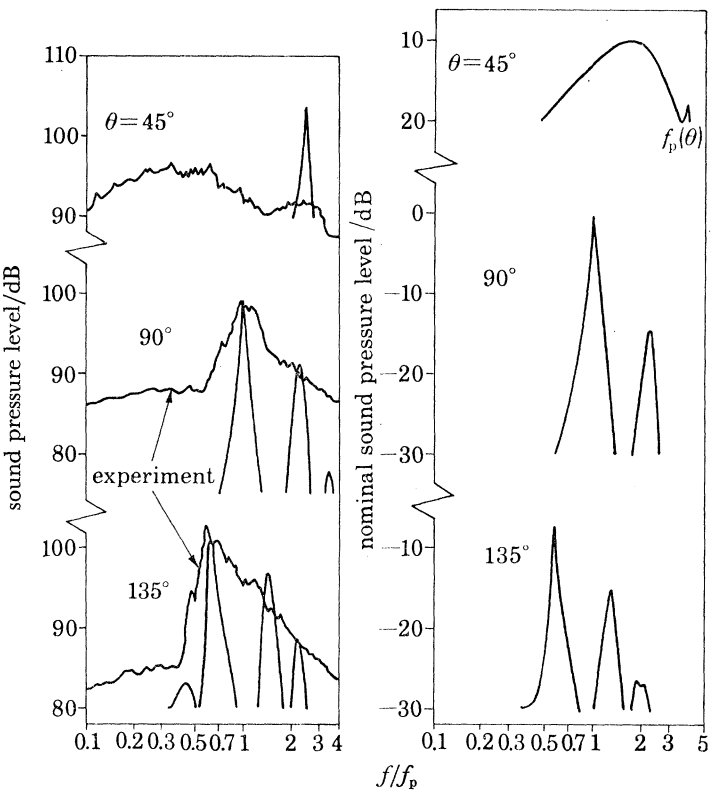

FIGURE 4

FIGURE 5

FIGURE 4. Comparison of experimental and theoretical shock associated noise spectra at three different angles θ to the jet axis. The shear layer width δ and the turbulence length scale l are adjusted to give an approximate fit to the experimental data at $\theta = 135°$. $l = 1.7$, $\delta = 0.02$.

FIGURE 5. Illustration of the predicted spectral shapes for a hot jet at the cut-back condition of table 1.

Each of the experimental spectra has a peak located approximately at $f = f_p(\theta)$, although in the rear arc ($\theta = 45°$) this principal peak is overshadowed by a broader maximum occurring at much lower frequencies. This additional strong contribution to the noise spectrum is likely to be associated with the known dominance of broad-band jet-mixing noise in the rear arc (see, for example, Tanna 1977); it is not inconsistent, however, with the field that must arise from the multiple scattering of the internally scattered wave modes in the manner discussed in §7. Note also that the second peak of the measured spectrum is just discernible above the background noise at $\theta = 90°$, 135°.

When interpreting the theoretical curves it should be borne in mind that in reality the eddy convection velocity V actually fluctuates randomly about a local mean value (say, for example, $0.6U$), and that this variation would manifest itself as a general broadening of the ideal spectral

peaks predicted by equation (10.11). This would tend to fill-in the deep valleys between the rather sharp peaks of the spectra. In this respect there is good agreement between the theoretical and experimental spectra at $\theta = 90°$. In the rear arc, at $\theta = 45°$, the theory greatly overestimates the shock-associated noise peak and exhibits no enhancement at the lower frequencies which was argued above to correspond to jet mixing noise. The large discrepancy at the peak radiation frequency may be ascribed to the increased importance of multiple scattering (neglected in the theory) on sound radiated in the downstream direction. This is because waves which propagate into the rear arc have a relatively short characteristic wavelength and are therefore more likely to be scattered by the expanding turbulent shear flow through which they must pass.

It is perhaps unwise to accept literally the apparent agreement between theory and experiment because of the unrealistically small shear layer width δ/a required in the comparison. However, the relative importance of the axial and radial acoustic dipoles discussed at the end of §8 is presumably correctly modelled by the theory.

In order to illustrate the predicted spectral shape for a hot jet, spectra have been plotted in figure 5 for the *Olympus* engine at the 'cut-back' condition of table 1 in the case in which $\delta/a = 0.1$ and $l/a = 1.5$. The general features are similar to those of the cold jet; for each value of θ the spectrum has a sharp peak at $f = f_{\mathrm{D}}(\theta)$. At $\theta = 45°$, however, the spectral level is greatly enhanced over a broad band of lower frequencies. This is similar to the experimental behaviour illustrated in figure 4 for a cold jet, although in the present case it cannot be associated with mixing noise. A numerical investigation reveals that it is directly attributable to the temperature difference between the jet and the ambient medium.

(ii) *Field shape of the direct scattered sound: effect of forward flight*

The sound pressure level $\overline{p^2}$ of the direct scattered field at the observer position (R, θ) is given by the integral (8.13). Taking account of the effect of finite shear layer width (§9) this becomes

$$\overline{p^2}(\theta) = \frac{P^2\beta_1^2 V^3 \rho_0}{\pi^2 R^2 U^4 \rho_1}\int_{-\infty}^{\infty} \frac{\Phi(\Omega/V)\, Z_1(\bar{k}, \Omega\cos\theta/c_0)\, J_1(\beta_1\bar{k}a)^2\,\mathrm{d}\Omega}{\Omega^2(1-M_0\cos\theta)^4|J_0(\beta_1\bar{k}a + \mathrm{i}\Delta_1(\bar{k}))|^2}. \tag{10.13}$$

The integral can be estimated by assuming that the dissipation function $\Delta_1(\bar{k})$ is sufficiently small that

$$\frac{J_1(\beta_1\bar{k}a)^2}{|J_0(\beta_1\bar{k}a + \mathrm{i}\Delta(\bar{k}))|^2} \approx \sum_{n=-\infty}^{\infty} \frac{\pi}{\Delta_1(\bar{k})}\delta(\beta_1\bar{k}a - \lambda_n) \tag{10.14}$$

By substituting into (10.13) and using the formula (10.6) for the dissipation function, it then follows that

$$\overline{p^2(\theta)} = \frac{2aP^2\beta_1^3 V^2(\rho_0/\rho_1)}{\pi R^2 U^4|1-M_0\cos\theta|^3}\sum_{n=1}^{\infty} \frac{\Phi\left(\dfrac{\lambda_n}{\beta_1 a(1-M_0\cos\theta)}\right) Z_1\left(\dfrac{\lambda_n}{\beta_1 a}, \dfrac{-M_0\lambda_n\cos\theta}{\beta_1 a(1-M_0\cos\theta)}\right)}{\lambda_n^2 \Delta_{1n}} \tag{10.15}$$

where

$$\Delta_{1n} = \Delta_1(\lambda_n/\beta_1 a).$$

At this stage we can usefully introduce a correction which takes account of the principal effect of subsonic aircraft flight. To do this we assign to the ambient fluid a velocity, U_{f}, say, in the positive x-direction. A complete analysis of the coherent structure of the jet is much more difficult in this situation because there now exists a coherent disturbance in the ambient medium. A precise specification of this disturbance would require a consideration of the diffracting effect of the nozzle. However, downstream of the nozzle the perturbed, coherent flow in the ambient medium

would be expected to resemble that of a jet if infinite extent. The bulk of the scattering of the steady shock cell wave system by the turbulence occurs in the downstream region and we shall therefore assume that an adequate modification of our formulae due to flight may be obtained by using that representation of the cell structure which obtains when the presence of the nozzle is ignored.

The structure of the *undamped* shock cells is given by the infinite series (2.11) in the absence of an ambient flow, and depends on the zeros λ_n of $J_0(z)$. When the ambient medium has velocity U_f, the displacement of the boundary of the jet is determined by the non-trivial zeros of a suitably modified form of the dispersion function (7.1) which defines the possible eigenmodes of a circular jet. In a reference frame which is *fixed relative to the nozzle* the wavenumbers k of stationary disturbances on the jet satisfy the following form of (7.1):

$$J_0(\beta_1 ka) - \operatorname{sgn}(k)\left(\frac{M_f}{M_J}\right)^2 \frac{\beta_1 \boldsymbol{K}_0(\beta_f|k|a)}{\beta_f \boldsymbol{K}_1(\beta_f|k|a)} J_1(\beta_1 ka) = 0, \tag{10.16}$$

where $\boldsymbol{K}_0$, $\boldsymbol{K}_1$ are modified Bessel functions (Abramowitz & Stegun 1965, p. 375), $M_f = U_f/c_0 < 1$ is the flight Mach number and $\beta_f = \sqrt{(1-M_f^2)} > 0$.

For small values of M_f the roots $\beta_1 ka \equiv \Lambda_n$, say, of this equation differ by a small amount from those governing the coherent wave system in the absence of flight. Define

$${}_nZ_f = \left(\frac{M_f}{M_J}\right)^2 \frac{\beta_1 \boldsymbol{K}_0(\beta_f|\lambda_n|/\beta_1)}{\beta_f \boldsymbol{K}_1(\beta_f|\lambda_n|/\beta_1)} \geqslant 0. \tag{10.17}$$

This quantity is always less than about 0.33 for $0 \leqslant M_f \leqslant 0.7$. It follows that when $\beta_1 ka$ is close to Λ_n the dispersion equation (10.16) may be approximated by

$$J_0(\beta_1 ka + {}_nZ_f \operatorname{sgn}(k)) = 0 \tag{10.18}$$

in which terms of order ${}_nZ_f^2$ have been discarded.

Hence we have in this case

$$\Lambda_n = \lambda_n - {}_nZ_f \operatorname{sgn}(n). \tag{10.19}$$

In the same approximation the modified structure of the coherent wave system is given by equation (2.11) with Λ_n replacing λ_n. Since $|\Lambda_n| < |\lambda_n|$ we deduce that the ambient flow increases the characteristic length of a shock cell and must accordingly diminish the peak spectral frequency f_p of the direct scattered sound. This result may also be incoporated directly into equation (10.15) for the sound pressure level by replacing λ_n by Λ_n in the summation.

To complete the specification of the effect of flight account must be taken of the Doppler shift in frequency produced by the ambient flow. This may be done by noting that in the presence of an ambient flow equation (8.5) which relates the frequency Ω relative to an observer at rest in the ambient medium to ω, that relative to the shear layer, becomes

$$\Omega = \omega + (V - U_f)\, K. \tag{10.20}$$

Similarly (8.6) is now

$$k \equiv \bar{k} = (-1/V)\{\Omega - (V - U_f)\, K\}. \tag{10.21}$$

The subsequent steps in the analysis of §8 leading to (8.13) are unchanged, and it follows finally that at a flight Mach number M_f the sound pressure level (10.15) becomes

$$\overline{p^2(\theta)} = \frac{2aP^2\beta_1^3 V^2(\rho_0/\rho_1)}{\pi R^2 U^4 |1-(M_0-M_f)\cos\theta|^3} \sum_{n=1}^{\infty} \frac{1}{\Lambda_n^2 \Delta_1(\Lambda_n/\beta_1 a)} \Phi\left(\frac{\Lambda_n(1+M_f\cos\theta)}{\beta_1 a[1-(M_0-M_f)\cos\theta]}\right)$$
$$\times Z_1\left(\frac{\Lambda_n}{\beta_1 a}, \frac{-M_0\Lambda_n\cos\theta}{\beta_1 a[1-(M_0-M_f)\cos\theta]}\right). \tag{10.22}$$

Note that forward flight of the aircraft alters the effective mean shear layer velocity V which is now increased in a manner which we shall assume to be described approximately by

$$V = 0.6(U - U_f) + U_f.$$

Also in (10.21) the polar coordinates (R, θ) refer to the position of the observer relative to the nozzle at *the time of emission of the sound*. This is the reference frame that is normally employed in aerodynamic noise studies.

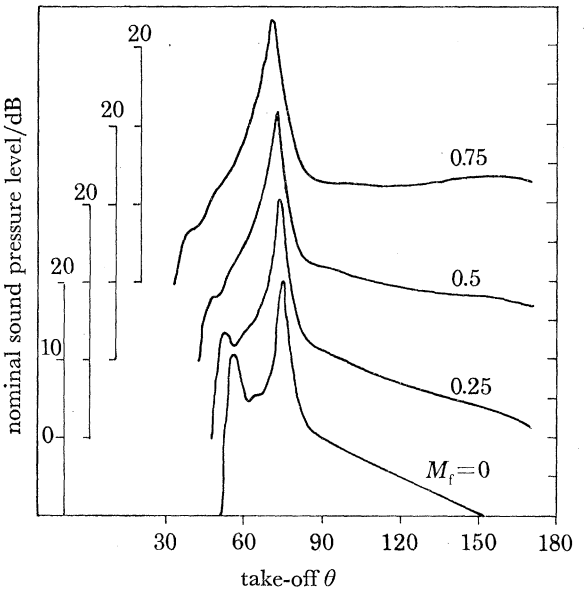

FIGURE 6

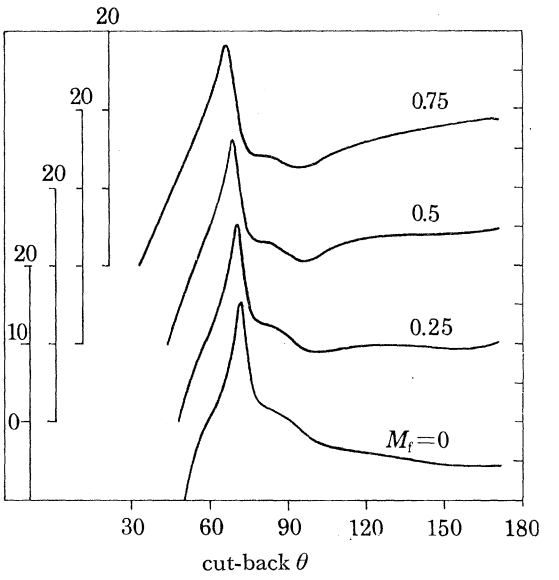

FIGURE 7

FIGURE 6. Illustration of the variation with flight Mach number M_f of the directivity of the direct scattered sound at the take-off condition of table 1 and for $l/a = 1.5$, $\delta/a = 0.1$.

FIGURE 7. As for figure 6, at the cut-back condition of table 1.

The variation in the field shape of the direct scattered sound predicted by (10.22) is illustrated in figures 6, 7 for a sequence of flight Mach numbers M_f, and in the particular case in which $\delta/a = 0.1$, $l/a = 1.5$. The sound pressure level $\overline{p^2(\theta)}$ is plotted in dB relative to $\overline{p^2(\theta = 90°)}$ at zero flight velocity, both for the take-off (figure 6) and cut-back (figure 7) conditions of the *Olympus* engine given in table 1.

The figures reveal a general rise in the forward arc radiation ($\theta > 90°$) with increasing flight Mach number. The peak radiation angle reduces from about 75° to 73° as M_f increases from zero to 0.75 at the take-off condition, the corresponding variation is from about 72° to 66° for the jet at the *Concorde* cut-back condition. Observe also that the predicted peak level is relatively insensitive to forward flight variations, and in general the effect of flight is minimal for directions lying between the peak angle and $\theta = 90°$.

The field shape predicted at the cut-back condition is particularly interesting. Deneuville (1976) has developed a prediction scheme for shock associated noise based on a series of model jet experiments involving a convergent nozzle with an exit diameter of 43 mm. The dotted curve in figure 8 shows the directivity predicted by Deneuville (Jacques 1977) at a distance of 78 nozzle

exit diameters for a jet of total temperature $T_J = 1100\,\mathrm{K}$ operating at a pressure ratio $p_J/p_A = 2.5$. (The prediction procedure is uncertain for θ less than the peak radiation angle and a dashed curve has been plotted in this region). This pressure ratio is close to that of the cut-back condition of table 1 and, in spite of the relatively large difference in the total temperatures (815 K rather than 1100 K), the corresponding theoretically predicted directivity (figure 7, $M_f = 0$) is not significantly different in shape from Deneuville's curve. This invites comparison of the absolute sound pressure levels under norminally identical jet conditions.

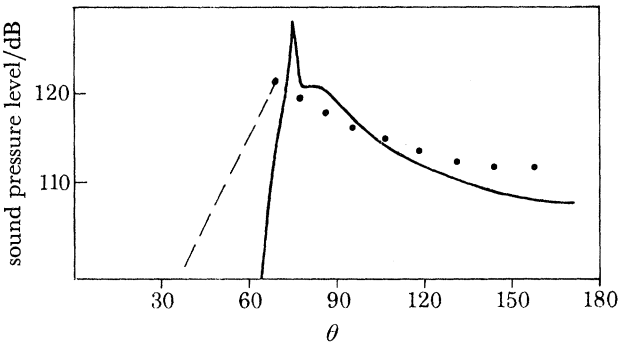

FIGURE 8. Comparison of static experimental and theoretical shock associated noise directivities for a jet at 1100 K operating at a pressure ratio of 2.5. ....., experiment (Deneuville 1976, quoted in Jacques 1977); ——, equation (10.15) with $\delta/a = 0.22$, $l/a = 2$, $V = 0.7U$, $\langle \xi^2 \rangle^{\frac{1}{2}} = 0.2U$.

The full curve of figure 8 represents the absolute field shape predicted by equation (10.21) at 78 nozzle exit diameters for $T_J = 1100$ K and $p_J/p_A = 2.5$. The level and shape of the theoretical curve depend on the values of the shear layer width δ, the turbulence length scale l, the eddy convection velocity V and the root mean square fluctuation velocity $\langle \xi^2 \rangle^{\frac{1}{2}}$. In figure 8 we have taken

$$\left.\begin{aligned} \delta &= 0.22a \\ l &= 2a \\ V &= 0.7U \\ \langle \xi^2 \rangle^{\frac{1}{2}} &= 0.2U \end{aligned}\right\} \tag{10.23}$$

which provide a reasonable fit to the experimental curve and are not expected to depart substantially from the representative values for a real jet. In this respect recall that in the theoretical model the vortex cores lie on the inner interface $r = a$ of the shear layer, so that the effective radial width of a typical eddy may arguably be taken as 2δ. We then have $l/2\delta = 4.55$ which is not substantially different from the mean spacing-to-width ratio of about 3.5 deduced by Moore & Saffman (1975) in an analogous situation involving incompressible flow.

No account has been taken in this comparison of the contribution to the sound pressure level from multiple scattering of the internally scattered wave modes (see §7). This can be significant provided that the energy of these modes is not substantially diminished by dissipation within the jet. It is possible that the free space radiation that results from multiple scattering has essentially the same directivity as the direct scattered sound, since it is produced by the same physical mechanism, and this would therefore tend to augment the theoretical prediction by raising the directivity curve by a uniform amount over all angles. A reduction in the value of l/a (for example) may be shown to reduce the absolute level predicted by equation (10.22). Accordingly a somewhat

smaller value of the eddy length scale l would be required to provide a satisfactory comparison with experiment when the internal modes are included.

We have seen above that forward motion of the aircraft modifies primarily the predicted field shape in the forward arc ($\theta > 90°$). It is customary to describe the effect of flight by means of a classical Doppler amplification formula of the form

$$\overline{p_i^2(\theta)} = F/(1+M_f\cos\theta)^n. \tag{10.24}$$

In the present discussion $F \equiv F(l/a, \delta/a)$ and the exponent $n \equiv n(l/a, \delta/a)$ would depend on the characteristic eddy length scale l and shear layer width δ, as well as the total jet temperature and the pressure ratio. It is hardly likely that such a simple equation can represent forward flight variations over a considerable range of θ and M_f. In practice, however, it is still useful to have an indication of the relevant value of the exponent n even for a relatively narrow range of variation of these parameters.

Equation (10.22) has been used to determine the mean value of n for $90° < \theta < 150°$ and for $0 \leqslant M_f < 0.5$. The computations were undertaken for $\delta/a = 0.1$, 0.2 and the results plotted against l/a in figure 9 for the three *Olympus* jet conditions of table 1. The curves do not determine n for systematic variations in total jet temperature and pressure ratio, but they indicate that a smaller Doppler amplification is associated with higher temperatures and pressure ratios. Doubling the width of the shear layer does not materially alter the value of n except when l/a is close to unity, and indeed it appears that for $1 < l/a < 3$, which is probably the practical range of interest, the variations in the exponent are not particularly significant. The values $n = 2.5$ and $n = 3.5$ may reasonably be said to characterize respectively the take-off/reheat and cut-back conditions of the *Olympus* engine.

(iii) *The total radiated sound power*

Let us now estimate the total radiated sound power associated with the presence of shock cells in an imperfectly expanded jet. The radiation comprises the direct scattered sound together with that due to the multiple scattering of the internally scattered random wave modes. Confine attention to the static case ($M_f = 0$). It has been argued in § 7 that the total power flux $\mathscr{P}$ into the random disturbances is given to a good approximation by

$$\mathscr{P} = \frac{\pi a^2 \beta_1^2 P^2 V}{2\rho_1 U^2}. \tag{10.25}$$

An upper limit to the total sound power may therefore be obtained by assuming that, before their scattering into free space, the dissipation of the random internal wave modes can be neglected. Equation (10.25) must then give the flux of energy into the ambient medium.

Recall that this expression for the power has been determined in a reference frame which is fixed relative to the mean shear layer, and which therefore convects at a velocity V relative to free space. The calculation of $p_t(\theta)$, the *total* far field acoustic pressure distribution, requires the consideration of a multiple scattering problem and is not determined by the analysis of this paper. On the other hand comparison with (8.12) shows that the following relation must hold between $p_t(\theta), \mathscr{P}$:

$$\mathscr{P} = \int [\overline{p_t^2(\theta)}/\rho_0 c_0]\,(1 - M_0\cos\theta)\,\mathrm{d}\Sigma, \tag{10.26}$$

where the integration is over the surface of a large sphere of radius R centred on the nozzle exit.

The effective total power $\mathscr{P}_T$ radiated into free space must be calculated in a coordinate system in which the ambient medium is at rest relative to the observer, and is given by

$$\mathscr{P}_T = \int [\overline{p_t^2(\theta)}/\rho_0 c_0]\, d\Sigma. \tag{10.27}$$

To estimate the value of $\mathscr{P}_T$ assume that

$$\left.\begin{aligned} \overline{p_t^2(\theta)} &= \text{const} \quad (\theta > \theta_p), \\ &= 0 \quad (\theta < \theta_p), \end{aligned}\right\} \tag{10.28}$$

where θ_p is the peak radiation angle discussed in (ii). Equations (10.26), (10.27) then yield

$$\mathscr{P}_T \approx \frac{\mathscr{P}}{[1 + M_0 \sin^2(\tfrac{1}{2}\theta_p)]}. \tag{10.29}$$

This result can be used with the data quoted in table 1 to predict the efficiency of the total shock associated noise of the *Olympus* 593 engine. The excess pressure P which appears in (10.25) may be estimated from the Bernoulli equation if the sonic point of the real jet flow is assumed to occur at the nozzle exit. The results of such a calculation, expressed as a ratio with the atmospheric pressure p_A, are given in the second column of table 2.

Define the total jet power $\mathscr{P}_J$ by $\mathscr{P}_J$ = thrust × exhaust velocity. Using conditions at the throat of the nozzle we have in the usual way that

$$\mathscr{P}_J = [2(\gamma - 1)/\gamma]\, Q C_p T_J. \tag{10.30}$$

Recalling that in the theoretical model $\pi a^2 = S$, the nozzle exit area, and that $V \approx 0.6U$, it follows from (10.25), (10.29) and (10.30) that the predicted shock noise efficiency is given by

$$\frac{\mathscr{P}_T}{\mathscr{P}_J} = \frac{15\gamma\beta_1^2 P^2}{(1 + M_0 \sin^2(\tfrac{1}{2}\theta_p))\,(\gamma - 1)\, M_J (Q/S)^2 C_p T_J} \left(\frac{2T_J}{(\gamma+1)\, T_d}\right)^{(\gamma+1)/2(\gamma-1)} \%. \tag{10.31}$$

By using the data of table 1 and taking $\theta_p = 70°$ this leads to the predictions of column 3 of table 2 for the shock noise efficiency of the *Olympus* engine. A comparison with experiment is provided by the final column of table 2 which lists the corresponding efficiencies (mixing noise plus shock associated noise) calculated from the experimental data of Hoch, Duponchel, Cocking & Bryce (1972), fig. 14).

TABLE 2

		percentage acoustic efficiency	
mode	excess pressure ratio, P/p_A	predicted (equation (10.31))	experiment (Hoch *et al.* 1972)
cut-back	0.29	0.17	0.48
take-off	0.63	1.08	0.93
re-heat	0.64	1.17	0.57

This comparison reveals a remarkable degree of order of magnitude agreement. The prediction formula (10.31) associates the greatest noise levels with higher total temperatures and pressure ratios. For the larger values of T_J and p_J/p_A, however, the experimental results exhibit a reduction in the overall efficiency (cf. 'take-off' and 're-heat'), which is related to the corresponding decrease in the density of the jet (see, for example, Hoch *et al.* 1972).

The above assumption that the dissipation within the jet of the internally scattered wave modes can be ignored, so that all of their energy eventually escapes into free space as sound, may well be a gross simplification. Static jet measurements (Harper Bourne & Fisher 1973; Tanna 1977) in the forward arc at $\theta = 135°$ indicate that the sound pressure level varies as β_1^4 for values of $\beta_1 \equiv \sqrt{(M_J^2 - 1)}$ in the range $0.5 - 1$. For the same range in β_1 it may be shown that the excess pressure $P \propto \beta_1^2$, and equations (10.25), (10.29) imply that the predicted sound power $\mathscr{P}_T$ scales on β_1^6. This difference could account for the systematic discrepancy between theory and experiment in table 2.

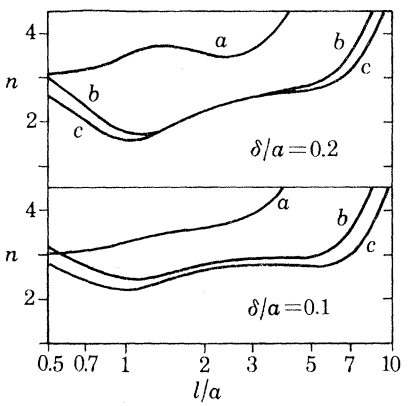

FIGURE 9

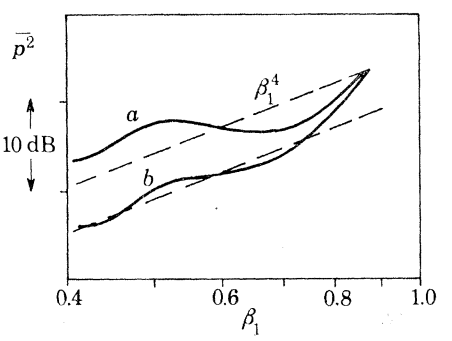

FIGURE 10

FIGURE 9. Variation of effective Doppler factor index of equation (10.24) as a function of the turbulence length scale l/a for two values of the shear layer width δ/a. (*a*) cut-back, (*b*) take-off, (*c*) re-heat condition of table 1.

FIGURE 10. Illustration of the variation of the direct scattered sound pressure level at $\theta = 135°$ as a function of $\beta_1 = \sqrt{(M_J^2 - 1)}$. (*a*) $T_J = 1100$ K, (*b*) $T_J = 813$ K; $\delta/a = 0.2$, $l/a = 2$.

In the extreme case in which the contribution from the internally scattered modes is neglected (or in which the total radiation is characterized by essentially the same law as that of the direct scattered sound, as implied in the discussion of figure 8), equation (10.22) may be used (with $M_f = 0$) to examine the dependence of the direct scattered sound on β_1. Figure 10 illustrates the corresponding variation of $\overline{p^2(\theta)}$ as a function of β_1 at $\theta = 135°$ for $\delta/a = 0.2$, $l/a = 2$, $V = 0.6U$ and for two values $T_J = 1100$ K, 815 K of the total jet temperature (cf table 1). We have argued in (ii) that these values of the model jet parameters are possibly representative of the real jet, and indeed the plots in figure 10 reveal a tolerable level of agreement with the observed β^4 law. Increasing/decreasing the width δ of the shear layer, however, tends to decrease/increase the effective exponent of the predicted power law dependence on β_1.

11. Summary of principal conclusions

In this paper we have examined in detail a theoretical model of the interaction between turbulent velocity fluctuations and the shock cell system of an imperfectly expanded jet. The jet is of arbitrary temperature, but no account has been taken of the temperature inhomogeneities which would then be present in the flow and also participate in the interaction. This is not expected to modify significantly the principal conclusions, which have been shown to depend only marginally on the details of the scattering mechanism, provided the interaction is weak.

It has been deduced from the theoretical model that:

(1) the scattered field consists of two essentially distinct components: (i) the direct scattered sound, which in the literature has hitherto been referred to as *the* shock associated noise; (ii) the internally scattered disturbances, which are probably primarily responsible for the decay of the shock cell system, and which give rise to a broad band spectrum of free space radiation.

(2) The directivity of the direct scattered sound (i) is essentially uniform over a wide range of angles in the forward arc, the peak radiation angle being at about 70° to the jet axis. Forward flight of the aircraft raises the forward arc radiation levels, corresponding to a Doppler amplification exponent of approximately 2.5 for the *Concorde* supersonic transport at the take-off/re-heat conditions, and 3.5 at cut-back, but hardly affects the radiation for angles between 90° and the peak radiation direction.

(3) The total sound power associated with the presence of shock cells has a predicted efficiency ranging between 0.2–1.2% for the engine of a supersonic transport at typical take-off conditions, in good agreement with experiment.

This work is performed as part of the Rolls-Royce research programme on high-speed jet noise and the company's sponsorship is gratefully acknowledged. The authors are indebted to Dr J. R. Jacques of SNECMA Noise Department for the provision of data used in § 10, and also to Mrs Judy Broadway who undertook the graph plotting and numerical computations.

References

Abramowitz, M. & Stegun, I. A. 1965 *Handbook of mathematical functions*. Dover.
Bishop, K. A., Ffowcs Williams, J. E. & Smith, W. 1971 *J. Fluid Mech.* **50**, 21–31.
Davies, P. O. A. L., Fisher, M. J. & Barrat, M. J. 1963 *J. Fluid Mech.* **15**, 337–367.
Deneuville, P. 1976 A simplified prediction scheme for the shock associated noise of a supercritical jet exhausting from a conical nozzle. SNECMA report YKA no. 5982/76.
Dowling, A., Ffowcs Williams, J. E. & Goldstein, M. E. 1978 *Phil. Trans. R. Soc. Lond.* A **288**, 321–349.
Emden, R. 1899 *Annln. Phys. Chem.* **69**, 426.
Frisch, U. 1968 Wave propagation in random media. In *Probabilistic methods in applied mathematics*, vol. 1. (ed. Bharucha-Reid). New York: Academic Press.
Grabitz, G. 1975 Über die Wellenlänge im rotationssymmetrischen stationären Überschallfreistrahl. In Max-Planck-Institut für Stromungsforschung Göttingen: Festschrift zum 50. jähringen Bestehen des Instituts, pp. 233–240.
Harper Bourne, M. & Fisher, M. J. 1973 The noise from shock waves in supersonic jets. AGARD CP-131 paper no. 11.
Hoch, R. G., Duponchel, J. P., Cocking, B. J. & Bryce, W. D. 1972 Studies on the influence of density on jet noise. First Int. Symp. on Air Breathing Engines, Marseille, 19–23 June 1972.
Howarth, L. (ed.) 1953 *Modern developments in fluid dynamics, high speed flow*, vol. 1. Oxford: University Press.
Howe, M. S. 1971 *J. Fluid Mech.* **45**, 769–804.
Howe, M. S. 1973 *Phil. Trans. R. Soc. Lond.* A **274**, 523–549.
Howe, M. S. 1975 *J. Fluid Mech.* **71**, 625–673.
Jacques, J. R. 1977 Efficiency of generation of shock associated noise. SNECMA report YKA No. 6081/77.
Landau, L. D. & Liftshitz, E. M. 1959 *Fluid mechanics*. Oxford: Pergamon Press.
Liepmann, H. W. & Roshko, A. 1957 *Elements of gasdynamics*. New York: J. Wiley.
Lighthill, M. J. 1952 *Proc. R. Soc. Lond.* A **211**, 564–587.
Lighthill, M. J. 1953 *Proc. Camb. Phil. Soc.* **49**, 531–551.
Lighthill, M. J. 1960 *Phil. Trans. R. Soc. Lond.* A **252**, 397–430.
Moore, C. J. 1977 *J. Fluid Mech.* **80**, 321–367.
Moore, D. W. & Saffman, P. G. 1975 *J. Fluid Mech.* **69**, 465–473.
Morgan, J. D. 1975 *Proc. R. Soc. Lond.* A **344**, 341–362.
Morse, P. M. & Ingard, K. U. 1968 *Theoretical acoustics*. New York: McGraw-Hill.
Munt, R. M. 1977 *J. Fluid Mech.* **83**, 609–640.
Pack, D. C. 1950 *Q. J. Mech. appl. Math.* **3**, 173–181.

PHILOSOPHICAL TRANSACTIONS OF THE ROYAL SOCIETY A MATHEMATICAL, PHYSICAL & ENGINEERING SCIENCES

Powell, A. 1953 *Proc. Phys. Soc.* B **66**, 1039–1056.
Prandtl, L. 1904 *Phys. Z.* **5**, 599–601.
Rayleigh, Lord 1916 *Phil. Mag.* (ser. 6) **32**, 177–187.
Stratonovich, R. L. 1963 *Topics in the theory of random noise*, vol. 1. Gordon & Breach.
Tanna, H. K. 1977 *J. Sound Vib.* **50**, 429–444.
Trevett, E. G. 1968 Velocity measurement in a jet from a convergent nozzle. Rolls Royce report AP 5531.

PHILOSOPHICAL TRANSACTIONS OF THE ROYAL SOCIETY A MATHEMATICAL, PHYSICAL & ENGINEERING SCIENCES